

HK-TN-91: HK LI Fibre Specifications

S.J. Jenkins, B. Bogdan, N. Foster, U. Limbu, N. ~~K.~~ McCauley

July 23, 2025

Contents

5	0 Version log	3
6	1 Introduction	4
7	2 HK LI System Overview	4
8	3 Laser System Specification	6
9	4 Fibre Lab Measurements	7
10	4.1 Fibre Test Stand	8
11	4.2 Preliminary Measurements	8
12	4.3 Attenuation Measurements	11
13	4.4 Dispersion Measurements	13
14	4.5 Fibre Choice	15
15	5 Fibre Switching Device	16
16	5.1 Overview	16
17	5.2 General Comparisons	16
18	5.3 Cross-talk Measurements	17
19	5.4 Summary	20
20	6 Speed of Light Measurements	20
21	7 Destructive Testing	20
22	7.1 <u>Crushing</u>	21
23	7.2 <u>Bending</u>	22
24	7.3 <u>Cutting</u>	22
25	7.4 <u>Scraping</u>	22
26	8 Reception Testing	22
27	9 Fibre Length Requirements	23
28	9.1 Injector Cell Locations	26
29	9.2 Fibre Paths	28

30	10 Photon Yield Requirements	40
31	11 Summary	42
32	A Additional Cross Talk Plots	46
33	A.1 Weinert FP400URT	46
34	A.2 Weinert GIF50C	47
35	B <u>Fibre Configuration</u>	48

36 0 Version log

- 37 • v1 - First release of TN, circulated to HK UK calibration group for comments.
- 38 • v2 - Updated to reflect comments received from HK UK calibration group. Also updated
39 photon yield requirements due to identified bug in WCSim simulation. This is the first
40 version made available to the collaboration.
- 41 • v3 - Fibre length requirements altered after deciding on specific injector cell locations. No
42 longer requiring all fibres to be the same length. Full description of injector cell locations
43 and fibre lengths given, as well as updating the laser system diagram to provide attenuators
44 individually for laser heads.
- 45 • v3.1 - Minor revision to make it clearer that different lengths of fibre in the barrel is the
46 primary approach.
- 47 • v3.2 - Minor revision after first review committee meeting. Added a section on reception
48 testing/QA/QC. Changed section on furcation tubing to reflect choice to tube all fibres,
49 this was outdated. Also fixed links to Thorlabs products (spec sheets seem to generate
50 limited-time URLs, now directing to the product page from which the spec sheets are linked).

51

52 1 Introduction

53 The Hyper-Kamiokande experiment has a broad physics program, including the aim of making
 54 precision measurements of neutrino oscillation parameters. In order to make such precision mea-
 55 surements, a precise understanding of the detector itself is required. To this end an array of
 56 different calibration systems are planned, with each playing a crucial role in driving systematic
 57 uncertainties down to the percent-level required.

58 A key component of the calibration program is the light injection (LI) system, which has two
 59 primary aims. The first is to measure the optical properties of the water in the tank, and monitor
 60 how the measured absorption and scattering parameters evolve with time. The second is to provide
 61 light sources with which to calibrate PMT response. In order to illuminate the injectors, lengths
 62 of fibre optic cable will be used to carry light from the sources on the top of the tank, all the way
 63 to the injectors installed on the PMT support structure.

64 This technical note focuses on the fibre optic requirements for the LI system, describing the
 65 quantities and lengths of cables needed, along with the lab measurements performed to decide on
 66 which types of fibre optic cables to use.

67 2 HK LI System Overview

68 The HK LI system will be split into two parts, one for the inner detector (ID) and one for the
 69 outer detector (OD). The ID system will consist of 33 injector positions, each housing a diffuser
 70 and collimator. Full details of the diffuser and collimator designs and requirements can be found
 71 in HK-TN-0042 [1] and HK-TN-0065 [2], respectively. Of the ID injectors, 28 will be located in
 72 the barrel region, with 7 locations equally spaced in z , each having four positions equally spaced
 73 in θ . The bottom end-cap will feature four more injector locations, with the injectors all facing
 74 upwards in the $+z$ direction. The top end-cap will feature a single location, where a calibration
 75 port will be used, rather than fixing to the PMT support structure. Figure 1 shows the injector
 76 locations described. Installing injectors at different heights throughout the detector will allow
 77 water parameters to be measured as a function of depth.

78 The OD system will consist primarily of diffusers, using bare hemispheres coupled to fibres,
 79 rather than the housed versions used for the ID system; 122 of these OD diffusers will be installed.
 80 The current design features 84 equally spaced around the barrel region. This results in 7 rows
 81 of 12 diffusers, with rows alternately offset from one another. This configuration is particularly
 82 advantageous as it matches the number of rows in the ID system, simplifying the installation of
 83 the fibre optic cables. Each end-cap would then feature 19 diffusers, again equally spaced across
 84 the surface. A diagram showing this layout is presented in Figure 2. Finally, 12 collimators will be
 85 installed in the OD, in suitable locations to achieve long path lengths such as across the end caps
 86 and up the side of the barrel. These collimators will be exactly the same as those installed in the
 87 ID.

88 In order to illuminate the injectors, two separate systems will be employed. The first of these
 89 will be a system formed of either five or six picosecond pulsed laser sources, in the wavelength
 90 range 337-550 nm. This laser system will be used to illuminate all of the ID injectors, along
 91 with the 12 OD collimators. The OD diffusers on the other hand will be illuminated by an LED
 92 pulser system, utilising a series of 365 nm wavelength LEDs. Both of these systems will feature

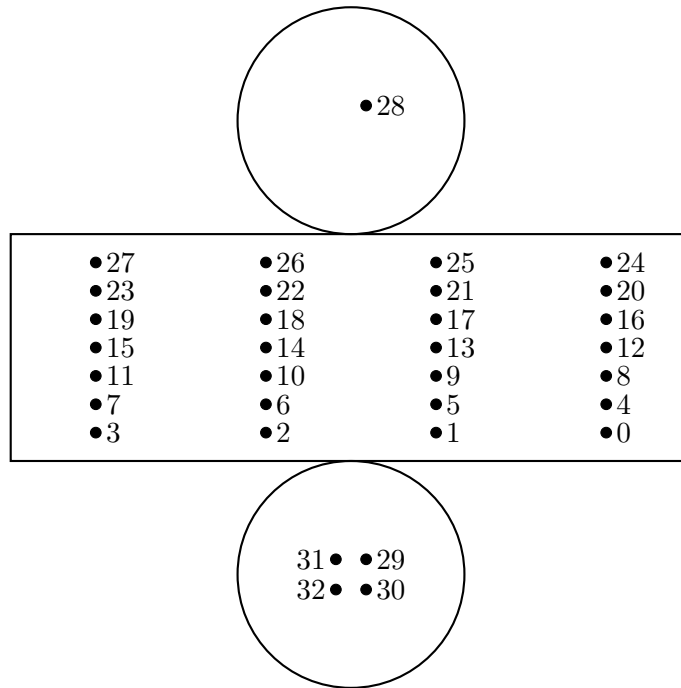


Figure 1: Injector location map for ID positions. Each location will feature a diffuser and collimator.

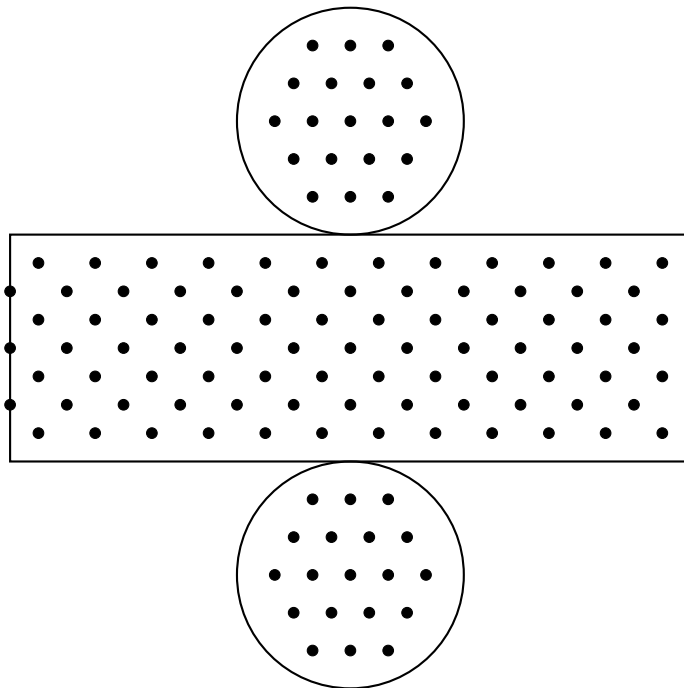


Figure 2: Injector location map for OD diffuser positions. Locations are approximate and dependent on PMT/WLS plate locations.

monitoring devices, so that the stability of the light sources can be monitored prior to convolution with detector parameters.

In total, including a laser diffuser ball and at least one spare channel, the lasers for the ID system will be required to couple to at least 80 channels. To accomplish this, dedicated fibre switching devices are required. A diagram giving an idea of the eventual laser and switch setup that would be used is given in Figure 3. These laser heads will be coupled into a single fibre using a 1-to-8

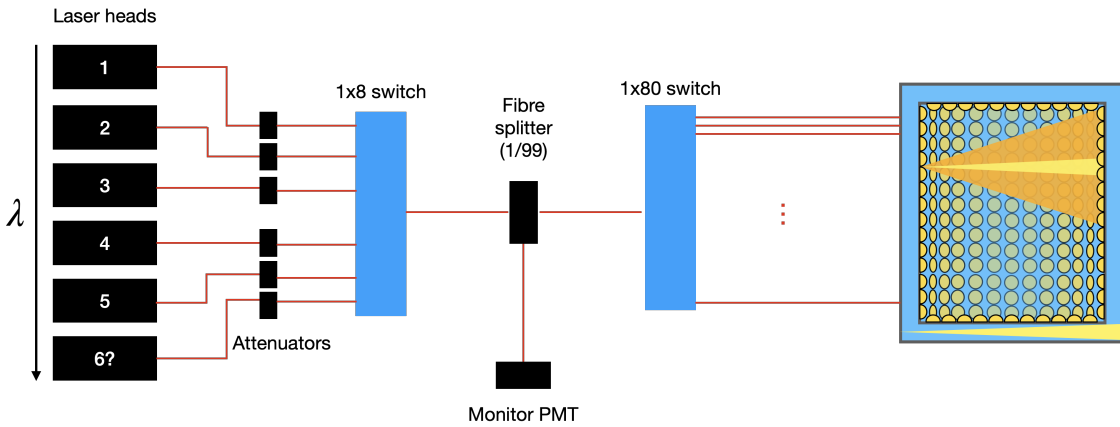


Figure 3: Diagram showing the likely setup for laser heads and fibre switchers.

99 (hereafter denoted as 1x8) switch, after each individually passing through air-gap attenuators.
 100 While only five laser heads are initially planned, this allows the system to be expanded at a later
 101 date if required. Individual attenuators are used so that the power can be manually tuned for each
 102 laser, independently of the others. The single fibre exiting the 1x8 switch can then connect to a
 103 fibre splitter with a 1/99 splitting. This allows 1% of the laser power to be directed to a nearby
 104 monitor PMT, which will monitor laser power before coupling into the long fibres and without
 105 entangling water parameters from within the detector. The fibre with the remaining 99% will go
 106 into a 1x80 switch, with the output going into the long fibres that extend down to the injectors.

107 3 Laser System Specification

108 In order to perform the desired calibrations across a range of wavelengths, a system of at least five
 109 pico-second diode lasers is required. These must ideally be controlled from a single unit, to simplify
 110 communication and operation during regular data-taking and dedicated calibration runs. These
 111 lasers should be fibre-coupled, to avoid the need to direct an open beam into the fibre system.
 112 Avoiding any open beams is also preferable in terms of safety to both users of the system, and any
 113 nearby workers. The intended setup for this laser system, as described in Section 2, is shown in
 114 Figure 3. While the setup will begin with five lasers heads, the switch will allow for up to eight to
 115 be connected, giving the ability to expand the system at a later date if required.

116 As the large lengths of fibre required to transport light from the laser sources to injection points
 117 will result in both attenuation and dispersion of the signal, output power and pulse width from
 118 the lasers should be maximised and minimised, respectively. The studies performed to estimate
 119 the required pulse energy to illuminate 1% of PMTs in spot region of each ID diffuser returned
 120 values of 5–10 pJ, with the maximum values at higher wavelengths. These studies are described in
 121 detail in Section 10. In certain scenarios, it will be necessary to inject more light into the detector
 122 than this. To account for this, a minimum pulse energy of 50 pJ was set for each laser wavelength.
 123 Coupling this with the requirement of short pulse widths, picosecond diode lasers were identified
 124 as the type of laser required. These lasers generally provide relatively high-powered pulses with
 125 pulse widths on the order of 1–100 ps.

126 Through our own market research and communicating with specialist laser suppliers, the pre-

ferred supplier identified for this system is PicoQuant [3], who manufacture high-powered pulsed picosecond diode lasers in a range of wavelengths. The Sepia PDL 828-L laser driver mainframe [4] allows for connection of up to eight laser drivers, which are all controlled from the single unit. This unit is capable of repetition frequencies with the internal oscillator of up to 80 MHz, though for the system in question triggering. The LDH Series of laser heads [5] provide pulses below 100 ps in length, in the wavelength range 375 to 1990 nm, with the option to run in pulsed or continuous mode. As an option, they can be fibre coupled, which as described will be necessary for the system. The laser heads which best fit the system requirements are the LDH-D-C-375, LDH-D-C-390, LDH-D-C-440 and LDH-D-C-500 [3], which provide peak wavelengths of 375 ± 5 , 395 ± 10 , 440 ± 10 and 500 ± 10 nm respectively. In order to go below 375 nm the LDH-FA Series of laser heads [6] can be used, which is a fibre amplified laser head, providing pulses of less than 80 ps in width. For this specific case, the LDH-P-FA-355 with peak wavelength at 355 ± 1 nm would be used. All of these laser heads fulfil the requirement of at least 50 pJ energy per pulse.

From this market research, it became clear that PicoQuant are the only company selling products that match the specification of both short pulse widths and high power. Several other companies which make picosecond diode lasers were contacted, but ultimately did not reach the power requirements. They are also fairly unique in the ability to control multiple laser heads with a single unit, whereas most commercial options need a single control unit per laser.

4 Fibre Lab Measurements

In order to make an informed decision on the optimal fibre optic cables to use for the LI system in HK, a series of measurements were made of the properties of the candidate fibres chosen. This section describes the fibre test stand setup at University of Liverpool, along with the measurements made of the candidate fibres, before discussing the decision on which fibres to use.

For the fibres to be suitable for use in the LI system, there are a series of requirements. These are:

- The fibre should be capable of transporting light of wavelengths in the range 337–550 nm.
- The attenuation of the input signal across the full length of fibre should be minimised.
- The dispersion of the input signal across the full length of fibre should be minimised.

Six different fibre types from Thorlabs were considered, to cover a range of options. Four of these were step-index fibres; two wide-core fibres (FP200URT [7] and FP400URT [8]) and two narrow-core fibres (FG050UGA [9] and FG105UCA [10]) were chosen. The remaining two candidates were graded-index fibres (GIF50C [11] and GIF50D [12]). Graded-index fibres were tested as it was expected that they would be required to limit dispersion of input signals across the full fibre length. It was particularly important to test the graded-index fibres as they are primarily for communications applications, and as such are only specified for operation above 800 nm. The main specifications of each fibre type are summarised in Table I. GIF50C and GIF50D have almost the same specifications, with the only difference being the available bandwidth. Preliminary measurements were performed with all six fibre types listed, and these results were used to make an informed choice on which should be investigated more thoroughly.

Fibre	Type	Core ϕ [μm]	NA	Transmission region [nm]
FG050UGA	Step-index	50	0.22	250-1200
FG105UCA	Step-index	105	0.22	250-1200
FP200URT	Step-index	200	0.50	300-1200
FP400URT	Step-index	400	0.50	300-1200
GIF50C	Graded-index	50	0.20	800-1600
GIF50D	Graded-index	50	0.20	800-1600

Table I: Fibre types used for initial testing in lengths of 1 m and 35 m.

166 4.1 Fibre Test Stand

167 All fibre measurements were performed using the fibre test stand in the Particle Physics Optical
 168 Laboratory at the University of Liverpool. Two different types of light sources are available for
 169 testing; the first of these is a Picoquant Sepia PDL 828-L laser driver [4], powering a LDH-D-C-
 170 375M laser head [5], with a peak wavelength of 371 nm. This is a pulsed laser source with a pulse
 171 width of \sim 50 ps, and repetition rate up to 80 MHz. The candidate fibres couple directly to the laser
 172 head using an FC/PC connector. The second set of light sources was a series of LEDs, covering
 173 wavelengths from 365 nm up to 595 nm. These are run in DC mode, and were used primarily
 174 to make attenuation measurements over the range of wavelengths relevant for the LI system. In
 175 order to connect the FC/PC connector on a candidate fibre to a surface-mounted LED, custom
 176 connectors were 3D printed.

177 Two different detection methods for the fibre transmitted light are available. To measure power
 178 output, a Thorlabs PM100USB [13] power meter is used, with an S150C sensor [14] connected.
 179 For timing measurements, the fibres are connected to a Hamamatsu H10721-210 PMT [15], which
 180 is read out by a Tektronix MSO54 oscilloscope [16]. Fibres are coupled to either read-out method
 181 via FC/PC connection such that, in the case of the laser, there are no bare beams in the lab.
 182 To ensure light tightness and as an additional safety measure, all light sources and detectors are
 183 housed within a dark box, with no connections made outside. Larger fibre reels are kept outside
 184 due to their size, with a port used to bring the ends inside for connection. An image of the setup
 185 is shown in Figure 4.

186 4.2 Preliminary Measurements

187 In order to narrow down the choice of fibre optic cable, all six options listed in Table I were
 188 purchased, in lengths of 1 m and 35 m. This is much shorter than the fibres that will be needed for
 189 Hyper-K; full length fibres were not used due to supplier issues. The length of cables which could
 190 be cut was limited by the size of the building used for production, as cold weather conditions during
 191 winter in the US at the time of ordering prevented them from being cut outside. Rather than delay
 192 the measurements, the decision was taken to start preliminary measurements of attenuation and
 193 dispersion with the lengths that were available.

194 4.2.1 Testing

195 Due to the early stage at which these measurements were made, the laser module described in
 196 Section 4.1 had not yet been set up. Instead, preliminary measurements of both attenuation and

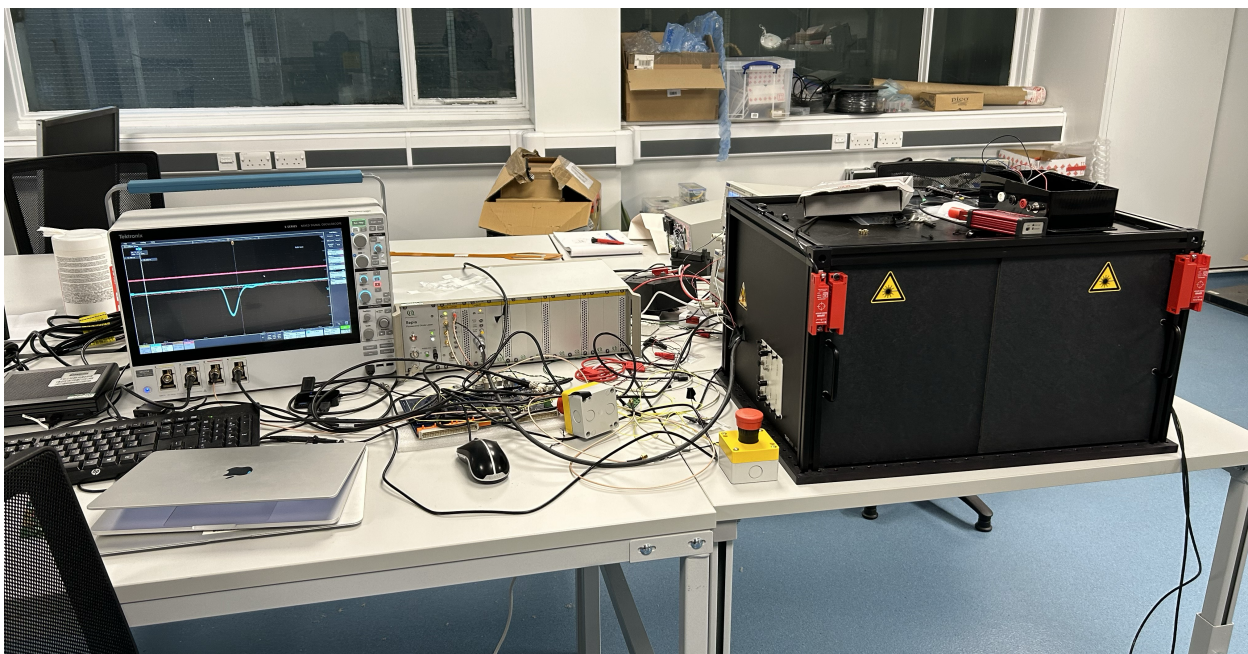


Figure 4: Fibre test stand in the optical lab at University of Liverpool.

dispersion were made using a pulsed 385 nm LED, operated by an early design of the LED pulser board that will be used for the OD LED system. In all tests, the 35 m lengths of fibre were left on the reels. This was both to remove cladding modes, as well as just to simplify the tests and not have to unwind this length of fibre around the lab. The 1 m fibres were also coiled to remove cladding modes as much as possible, though with such a short length the amount this could be done was limited.

To calculate dispersion of the signal across the fibre length, the width of the PMT signal pulse was measured for both lengths of each fibre. The pulse width is defined as the time elapsed while the voltage is at greater than 50% of the peak. A total of 20,000 measurements were made for each set to estimate the uncertainty. Subtracting these values in quadrature obtains the amount of dispersion observed. The pulse widths at both lengths and calculated dispersion values for each fibre are presented in Table II. The results shown here are mostly unsurprising. As expected, the

Fibre	Pulse width at 1 m [ns]	Pulse width at 35 m [ns]	Dispersion [ns]
FG050UGA	3.486 ± 0.111	4.207 ± 0.305	2.355 ± 0.569
FG105UCA	3.734 ± 0.075	4.841 ± 0.205	3.081 ± 0.335
FP200URT	3.809 ± 0.045	5.117 ± 0.158	3.416 ± 0.242
FP400URT	4.329 ± 0.054	5.252 ± 0.116	2.974 ± 0.219
GIF50C	3.453 ± 0.103	3.867 ± 0.260	1.741 ± 0.613
GIF50D	3.407 ± 0.101	3.899 ± 0.213	1.896 ± 0.509

Table II: Pulse width and dispersion values for initial fibre measurements, using a 385 nm pulsed LED source.

two graded-index fibres show the smallest amount of dispersion; this is exactly the reason they were added for consideration. For the first three step-index fibres, the dispersion increases with increased core diameter. However, it can be seen that the FP400URT, which has the largest core diameter, actually has a smaller amount of dispersion than the FP200URT. The typical rise time

213 of a 50 cm PMT is quoted to be 5 ns [17], so the fact that the pulse widths for all fibres but
 214 FP400URT are below this is a good sign.

215 The same set-up was also used to make preliminary measurements of attenuation in the fibres.
 216 As this was an early version of the fibre test stand, an optical power meter was not used. Instead,
 217 the area under the curve of each recorded pulse was used as a proxy, as this is proportional to the
 218 total charge collected by the PMT per pulse. Again, 20,000 measurements for each fibre sample
 were taken, and the results for this are presented in Table III. Again, the results shown here

Fibre	1 m [nVs]	35 m [nVs]	Transmittance [%]
FG050UGA	1.86 ± 0.23	0.75 ± 0.23	40.3 ± 13.3
FG105UCA	7.16 ± 0.62	4.17 ± 0.28	58.2 ± 6.4
FP200URT	16.53 ± 0.99	9.59 ± 0.74	58.0 ± 5.7
FP400URT	23.56 ± 1.14	19.24 ± 0.94	81.7 ± 5.6
GIF50C	4.61 ± 0.69	4.09 ± 0.59	88.7 ± 18.4
GIF50D	2.39 ± 0.57	0.56 ± 0.24	23.4 ± 11.5

Table III: Area-under-curve measurements from oscilloscope for 1 m and 35 m fibres, with calculated transmittance values.

219
 220 are unsurprising for the step-index fibres, with the transmittance increasing with increased core
 221 diameter. It can also be seen that the recorded values through the 1 m patch cable increase with
 222 increasing core diameter; this shows the difficulty of coupling particularly narrow-core fibres to an
 223 LED, which generally have a wide opening-angle for the light profile. The results obtained for the
 224 two graded-index fibres are seen to be very different, which is potentially related to the different
 225 bandwidths they're designed for, and the fact they're not specified for a wavelength range below
 226 800 nm. The amount of charge collected from a 1 m fibre for either of these types is again small
 227 due to them having a 50 μm core diameter, and suggests as expected that narrow-core fibres are
 228 not suitable for the OD LED pulser system.

229 4.2.2 Results

230 The results from these initial tests suggest that different fibre types will need to be employed for
 231 the ID laser and OD LED systems. For the OD LED system, where coupling the fibre to the LED
 232 and maximising light transmission is important, a wide-core fibre should likely be chosen. The
 233 FP400URT fibre showed the best transmission and input light acceptance, so this is the candidate
 234 that was favoured. For the laser system timing is more important; the dispersion measurements
 235 suggested that the graded-index GIF50C and GIF50D fibres were the best candidates here.

236 As this was a preliminary version of the fibre test stand, and measurements were carried out
 237 with fibre lengths significantly shorter than what will actually be installed into Hyper-K, the
 238 decision was initially taken to purchase three candidate fibres for further testing. These were
 239 FP400URT, GIF50C and GIF50D. Based on estimates of the length required, reels of 40 m and
 240 105 m length were purchased for each of these fibre types. However, it was later understood that
 241 the feed-throughs for the injectors would use an FG105UCA patch cable. In order to not add extra
 242 inefficiencies to the system in coupling different fibres to one another, the ideal scenario would
 243 be to use this fibre for the laser system. A reel of 105 m for this was also purchased and tested,
 244 with results for all four primary candidate fibres described together in the following sections for

245 simplicity.

246 4.3 Attenuation Measurements

247 4.3.1 Method

248 The full laser setup for the HK LI system will feature a minimum of five laser heads, over a range
 249 of wavelengths spanning UV to visible. In order to confirm whether attenuation in the candidate
 250 fibres is of an acceptable level across multiple wavelengths, LEDs across a series of wavelengths
 251 were used for these tests. Those were: 365, 395, 415, 465, 496, 525 and 560 nm. As timing is not
 252 relevant to attenuation measurements, and to ensure results were valid by initially getting enough
 253 light into the fibres, these LEDs were powered with a DC source.

254 Measurements were made of the output power from fibres of length 1, 2, 37, 42, 77, 107 and
 255 147 m, where some of these lengths were formed by coupling together multiple fibres of shorter
 256 length, and all lengths above 1 m featured two 1 m patch cables in the setup. To connect fibres
 257 together, FC/PC to FC/PC mating sleeves were used, which are quoted to have < 0.5 dB insertion
 258 loss [18]. As a 40 m length of FG105UCA fibre was not ordered, the measurements for this were
 259 done at slightly altered lengths. Power measurements were made using an optical power meter,
 260 as described in Section 4.1. The longer reels of fibre were purchased without tubing, and it was
 261 observed during data taking that there was some level of light leakage into the fibres, causing
 262 non-zero readings when the LEDs were not powered. To mitigate this, all measurements were
 263 performed with the reels of fibre that were too big to fit inside the dark box wrapped in black
 264 sheet.

265 The power observed after transmission through a fibre of length x can be written as

$$266 P = P_0 \exp^{-\lambda x}, \quad (1)$$

267 where P is the observed power after traversing the fibre, P_0 is the initial power, and λ is the
 268 coefficient of attenuation, describing how much attenuation occurs per unit length. Taking the
 269 natural logarithm of this,

$$270 \ln P = -\lambda x + \ln P_0, \quad (2)$$

271 allows a linear fit to be made to data, where the gradient is the coefficient of attenuation, and
 272 the y-intercept the log of the input power. The fitted attenuation coefficient can then be used to
 273 calculate attenuation in dB for a given fibre length, where in this case a length of 150 m is used:

$$274 \text{Attenuation (dB/150 m)} = \frac{10}{\ln 10} \times 150 \times \lambda. \quad (3)$$

275 4.3.2 Results

276 As a first check of the measurement system, the calculated attenuation values for the FP400URT
 277 fibre were compared to those provided in the fibre specifications by Thorlabs. This comparison can
 278 be seen in Figure 5, and shows generally good agreement between the two. Values of attenuation
 279 stay below 10 dB until just above 400 nm, where the amount of attenuation increases sharply.
 280 At the minimum wavelength of 365 nm, attenuation of over 20 dB is observed, suggesting that

281 attenuation values in the UV range will likely be the driving factor for deciding on a fibre type.

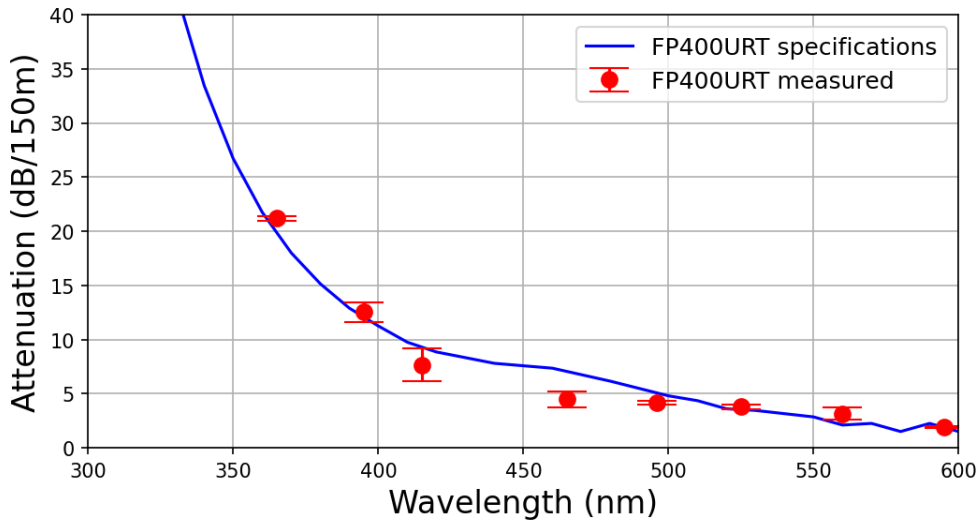


Figure 5: Measured attenuation scaled to 150 m length as a function of wavelength for the FP400URT fibre, compared to specifications from Thorlabs [8].

282 The full results for all fibre types are presented in Figure 6, with all values of attenuation again
 283 scaled to what would be seen across 150 m of fibre. As was shown for the FP400URT fibre, the
 284 amount of attenuation observed in the fibres peaks at the lowest wavelength scanned, 365 nm. At
 285 this value there is a large range of values observed, with the FG105UCA fibre exhibiting the lowest
 286 attenuation at under 15 dB. Conversely, the two graded index fibres show much greater attenuation.
 287 The spread of values at 395 nm is much reduced, with the two graded-index fibres instead exhibiting
 288 lower attenuation here. Above 400 nm, the FG105UCA fibre is seen to consistently exhibit higher
 attenuation than the other fibres, though in all cases is still below 10 dB. These results suggest that

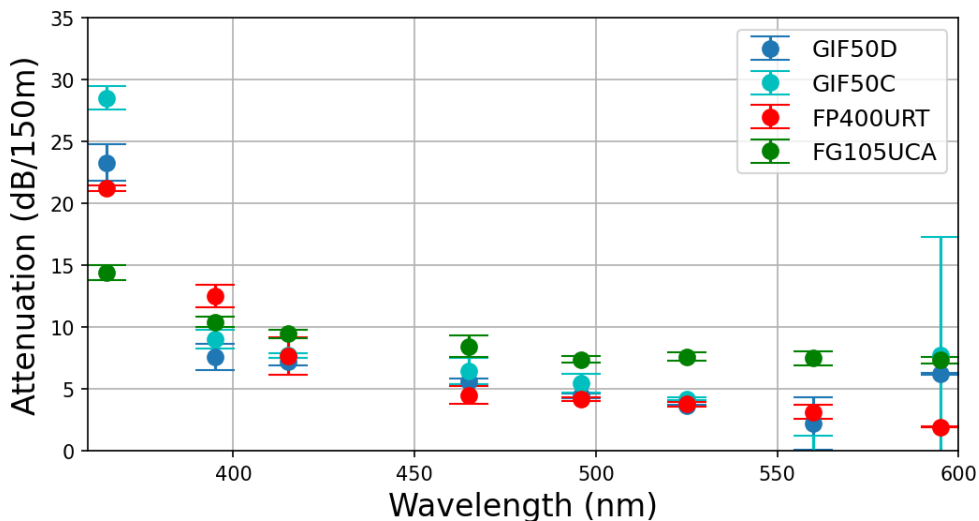


Figure 6: Measured attenuation scaled to 150 m length for all four candidate fibre types, as a function of wavelength.

289
 290 FG105UCA is the optimal fibre type to use, in terms of attenuation. Although it exhibits higher
 291 attenuation in the visible range, there is significantly less observed in the UV range, whereas the

292 other fibre options start to peak sharply in attenuation here. As lower wavelengths of light have
293 been previously observed to be more sensitive to changes in water parameters [20], prioritising
294 lower attenuation in this region should be preferred.

295 Performing these tests also provided an opportunity to become familiar with handling the fibres.
296 As was mentioned in Section 4.3.1, the long reels of fibre that were purchased for these tests were
297 done so without tubing, which is generally added in order to protect the fibres. Along with the
298 issues of light leakage previously discussed, during testing it was found that the narrow-core fibres
299 were particularly fragile, with two being broken in the process. The FP400URT fibre however
300 was seen to be far more robust and light-tight. This is attributed to its hard polymer cladding
301 and Tefzel (Teflon-based) coating, as opposed to the clear acrylate used for the graded-index and
302 FG105UCA fibres. ~~Orders of fibre types other than FP400URT will require tubing when ordered for the safety of the system. Despite this, for safety and light-tightness both types of fibres will use furcation tubing. The majority of fibres will be tubed using the Thorlabs FT030-BK black tubing [19]. This is the same tubing used on the fibres in the UK Light Injection (UKLI) system in Super-K, so it is known to be compatible with both ultra-pure and gadiated water. Short patch fibres used inside the LED pulser crate (described further in Section 9.2.5) will use different colours, associated with the different total fibre lengths that each pulser is connected to.~~

309 **4.4 Dispersion Measurements**

310 **4.4.1 Method**

311 Similarly to the attenuation measurements described above, by the time the full lengths of fibre
312 had been ordered in, the full fibre test stand had been commissioned. Importantly, this included
313 setup of the laser system described in Section 4.1, which was used as the light source for these
314 measurements. Instead of the $\mathcal{O}(\text{ns})$ input pulse provided by the pulsed LEDs in Section 4.2.1, the
315 laser delivers a pulse of width $\sim 50 \text{ ps}$, meaning measurements would not be limited by this.

316 Various lengths of each fibre were connected in turn to the laser head, in the same way as
317 in Section 4.3.1. However, due to breakage in the attenuation testing GIF50C was not included
318 in these tests. To make timing measurements, the fibres were connected to the PMT, where the
319 signal was visualised on the oscilloscope. Across 20,000 recorded pulses, measurements were made
320 of the pulse width, negative rise time and negative fall time. Pulse widths were again defined as
321 the time above 50% of the peak voltage, while rise and fall times were defined as the time between
322 20% and 80%, or vice versa.

323 In making these measurements, another limitation of the setup became apparent; it was clear
324 from initial measurements that the measured pulse width and rise time were highly dependent on
325 the amount of light detected by the PMT. This was understood to be a limitation caused by the
326 rise time of the PMT; shorter fibres which would deliver more light due to decreased attenuation
327 exhibited longer pulse widths, as the PMT response was not quick enough. In order to get around
328 this, the measurement approach was modified. For each length of fibre tested, the laser intensity
329 was adjusted such that the output pulse would deliver approximately the same peak voltage each
330 time. This should ensure that the rise time of the PMT had no impact on the timing measurements.

331 Another issue was encountered with this setup. When making measurements with the 1 m
332 patch cable, large tails in the pulses were observed. An example of this for the FP400URT 1 m

333 cable is shown in Figure 7. Here, negative rise time and negative fall time are labelled as fall time
 and rise time, respectively, due to the inverted nature of the pulse. It can be seen that the very

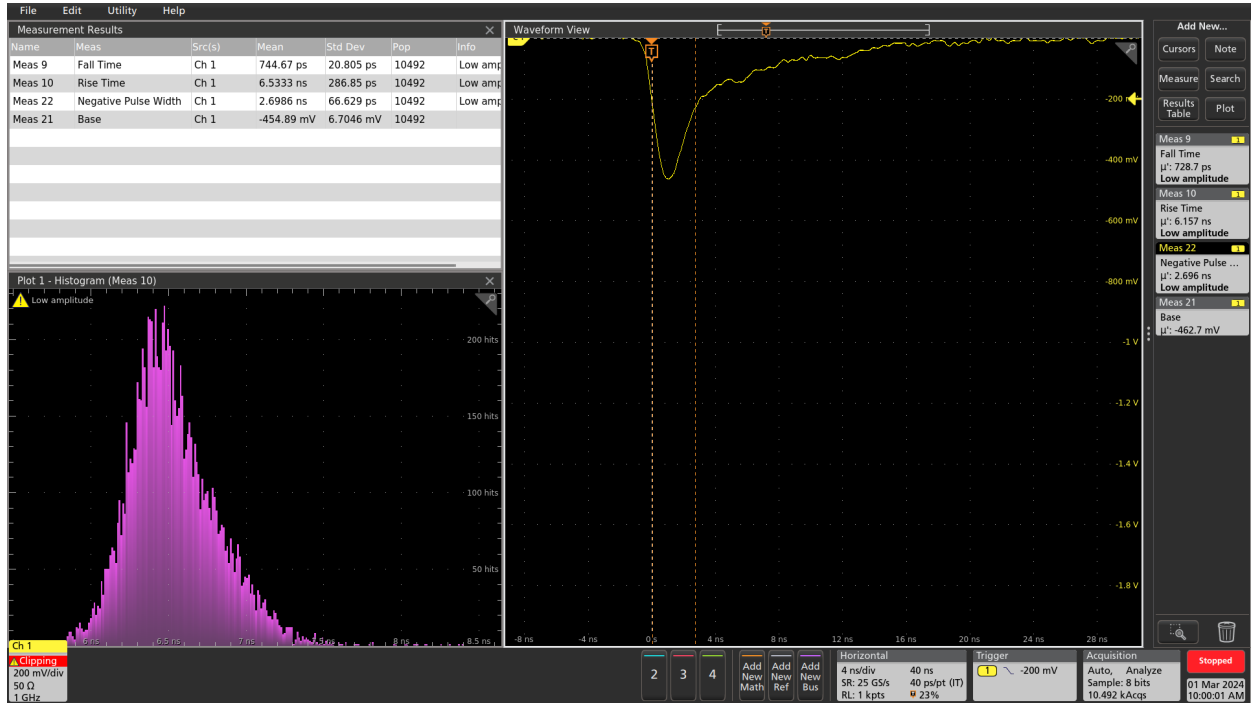


Figure 7: Scope trace and associated measurements for a 1 m FP400URT patch cable, showing the long falling tail observed.

334 slowly falling tail results in a negative fall time of 6.53 ± 0.29 ns, despite a negative rise time of only
 335 0.74 ± 0.02 ns. This results in a measured pulse width longer than those observed for longer fibre
 336 lengths, making dispersion incalculable. As the long tails diminish with increased fibre length, it is
 337 thought that they are caused by reflections at the fibre coupling faces. In order to not be affected
 338 by this, measurements instead focused on the negative rise time of pulses. Unfortunately this still
 339 makes dispersion incalculable, but at least gives a way to compare pulse timing for each fibre type.
 340

341 4.4.2 Results

342 The obtained rise time measurements for the three fibre types tested are given in Figure 8. As
 343 expected from the preliminary measurements, the fibre which exhibited the least increase in rise
 344 time was the graded-index, GIF50D, with an increase of 0.24 ± 0.03 ns. This is closely followed
 345 by FP400URT, which shows an overall increase of 0.34 ± 0.03 ns. A comparably higher increase
 346 is then observed for the FG105UCA fibre of 0.60 ± 0.05 ns. An interesting observation in these
 347 measurements is that the rise time increase is relatively sharp over the first ~ 50 m, but then
 348 plateaus toward the longest distances measured. This suggests that, should fibres be required to
 349 be longer than those tested, there should not be a substantial increase in rise time over what has
 350 already been observed. It should also be noted that, at the maximum distance of ~ 140 m, the
 351 measured rise times for all fibres are smaller than the typical 50 cm PMT rise time of 5 ns [17].

352 While these measurements give a good estimate of how timing will increase over large lengths
 353 for each fibre type, it will be important to confirm exact dispersion measurements for the chosen
 354 fibre type. As such, a high frequency readout system is currently in development, so that these

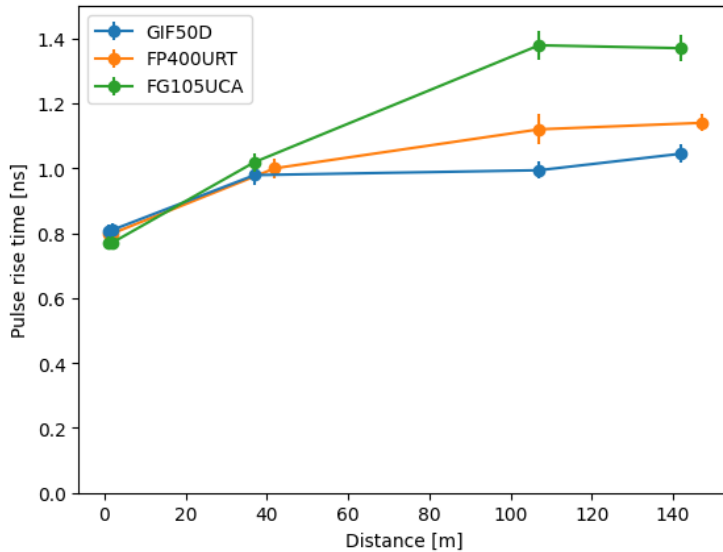


Figure 8: Pulse rise time measurements for three candidate fibres, across a range of lengths.

355 measurements can be made at a later time.

356 4.5 Fibre Choice

357 Unfortunately, the results from both the attenuation and dispersion tests are diametrically opposed;
 358 while the graded index fibres performed best in terms of dispersion and pulse rise time increase,
 359 they exhibited the greatest amount of attenuation. The opposite is true for the FG105UCA fibre,
 360 with FP400URT performance in the middle for both tests, meaning there is not a single fibre type
 361 that is clearly preferred. Specific aspects and requirements of the two separate LI systems should
 362 be taken into account to make this choice.

363 Firstly, it is important to remember that the decibel scale is logarithmic, meaning that the
 364 ~ 10 dB difference between the FG105UCA and FP400URT/GIF50D fibres observed at 365 nm
 365 represents an additional $\mathcal{O}(10)$ times power loss. Therefore, the differences observed in attenuation
 366 are much greater than for the pulse width measurement, and as such the former should be prioritised
 367 as a basis for fibre decisions. While the GIF50D fibre showed the best results in terms of rise time
 368 increase, it showed significantly worse attenuation. Secondly, the ID injectors (and OD collimators)
 369 already have an internal patch fibre of FG105UCA. Coupling a wide-core fibre such as FP400URT
 370 into this narrow-core fibre will result in significant light loss at the connection point, and so should
 371 be avoided. Therefore, on balance, the FG105UCA narrow-core step-index fibre is judged to be
 372 the optimal choice for the laser system. However, the initial results for the 1 m patch cables given
 373 in Table III make it clear that coupling an LED to such a small core diameter fibre is difficult. As
 374 such, the choice for the OD LED system is the FP400URT fibre, which has a four times wider core
 375 and the next best attenuation results.

376 5 Fibre Switching Device

377 5.1 Overview

378 As was mentioned in Section 2, the ID laser system will require dedicated fibre switching devices
 379 in order to couple all lasers to all possible channels. To that end, two potential companies that
 380 manufacture fibre switching devices were identified, and test devices in a 1x4 configuration were
 381 purchased for evaluation. From the first company, Agiltron [21], a single 1x4 device was purchased
 382 with FP400URT as the internal fibre. A second company, Weinert Industries [22] supplied two 1x4
 383 devices; one of these contained FP400URT fibre, while the other used GIF50C. All three devices
 384 are controlled via USB. It should be noted that only two companies could be found that could
 385 supply these kinds of specialist devices.

386 5.2 General Comparisons

387 To understand the performance of the three test switches, power measurements were made com-
 388 paring the output power from each of the four ports to a reference fibre of the same type. For the
 389 reference fibre measurements, two 1 m patch cables were coupled together to make a 2 m cable,
 390 with the total cable length of each of the switches being around this length.

391 Measurements were made using the 371 nm laser as the light source. The power meter was used
 392 to make measurements across 20,000 readings, where each of the four fibre outputs on a switch
 393 were selected and coupled to in turn. Power readings and calculated transmission percentages
 for the Agiltron FP400URT switch are given in Table IV. The results obtained show generally

	Agiltron FP400URT		Weinert FP400URT		Weinert GIF50C	
	Power (μW)	% of ref.	Power (μW)	% of ref.	Power (μW)	% of ref.
Reference	9.58 ± 0.01	100	9.67 ± 0.01	100	9.69 ± 0.01	100
Port 1	8.93 ± 0.01	93.11 ± 0.14	7.41 ± 0.01	76.64 ± 0.13	9.49 ± 0.01	98.09 ± 0.20
Port 2	8.67 ± 0.01	90.55 ± 0.14	7.41 ± 0.01	76.64 ± 0.13	9.59 ± 0.01	98.83 ± 0.20
Port 3	8.71 ± 0.01	91.06 ± 0.14	7.27 ± 0.01	75.18 ± 0.13	9.36 ± 0.01	96.70 ± 0.20
Port 4	8.66 ± 0.01	90.50 ± 0.14	7.00 ± 0.01	72.39 ± 0.13	9.23 ± 0.01	95.30 ± 0.20

Table IV: Power transmission across the 1x4 switching devices, with comparison to a reference cable of the same type as the device internal fibre.

394
 395 good power transmission for all three devices tested, albeit with clearly better transmission for
 396 the Agiltron FP400URT and Weinert GIF50C than for the Weinert FP400URT. This may be in
 397 part due to the fact the fibre on the Weinert FP400URT is longer than the others (and the 2 m
 398 reference), measuring approximately 2.3 m in total. It should be noted here that, at least for the
 399 Weinert switches, any switch with more than four outputs is formed by daisy-chaining together
 400 1x4 switches. For example, a 1x16 switch would be constructed by connecting the four output
 401 channels of a single 1x4 switch into the inputs of four additional 1x4 switches. Therefore for the
 402 required 1x6 and 1x80 switches, these losses will be experienced up to six times in total. It is
 403 unclear whether the Agiltron switch is constructed in the same manner.

404 The variation in output power between ports is also generally low across the devices, with a
 405 difference of 2.61% for the Agiltron FP400URT, 4.25% for the the Weinert FP400URT and 3.53%

406 for the Weinert GIF50C. These results suggest that the Agiltron device minorly outperforms the
407 Weinert devices in terms of power variation across ports, whilst the Weinert GIF50C was best for
408 transmission.

409 During ordering, setup and testing of these devices, we experienced very different degrees of
410 assistance from the two companies. While this is not a quantifiable metric, it is none the less very
411 important to keep in mind when making a decision for the full fibre system. The Agiltron switch
412 arrived with no documentation on how to set up and run the device. The correct way of doing this
413 was eventually understood out after several emails to the supplier. The Weinert switches on the
414 other hand arrived with full documentation, along with a simple software package for operation.
415 All email communication with them throughout the ordering and testing process has been very
416 helpful, if somewhat slow at times.

417 The LI system is a critical component of the HK calibration programme, and will need to
418 run for many years. It is crucial that support is available from the manufacturer of significant
419 components such as the fibre optic switch, should anything go wrong during its lifetime. The
420 experience of working with Weinert was significantly better, and this should be kept in mind when
421 selecting which device to proceed with. In particular, should issues arise with hardware in the
422 future, it would be significantly easier to deal directly with the manufacturer, rather than going
423 through a third-party distributor as with Agiltron.

424 **5.3 Cross-talk Measurements**

425 While making the transmittance measurements shown in Table IV for the Agiltron device, it was
426 noted that small non-zero readings were being made by the power meter whilst connected to ports
427 that were not currently being illuminated. These persisted after turning off the laser and re-zeroing
428 the power meter, and suggested some crosstalk between fibres. This is of course something that
429 should be avoided, as only one injector should be illuminated within the tank at a time.

430 In order to confirm this was the case and measure the level of crosstalk for these devices, four
431 power meters were set up, with one connected to each of the four ports on a switch, and all re-
432 zeroed at the same time. A simple python script was used to loop through the four ports 1000
433 times, before stopping at each port in turn and taking readings for ~ 10 s. This was repeated for
434 runs of approximately 18 hours per fibre switching device. Data was analysed by stripping out
435 data points from the rapidly varying periods, as well as the first and last point of each sustained
436 period where the device may still have been switching and thus not illuminating the port for the
437 entire time taken for one reading.

438 Data from this test is shown in Figures 9, 10 and 11 for the Agiltron FP400URT, Weinert
439 FP400URT and Weinert GIF50C switches, respectively. Each of these shows data taken by the
440 power meters when the port was a) illuminated and b) not illuminated. These plots show a
441 subset of the full data-taking runs in order to better show the observed structure. Figures 9a, 10a
442 and 11a, which show the readings from illuminated ports, show a similar level of variation to the
443 data presented in Table IV. The most interesting result is seen in Figure 9b, which shows clear
444 changes in the power readings recorded on ports 1 and 2, when these ports are not illuminated.
445 There is also a repeating structure to the data from port 4 suggesting a lower level of crosstalk
446 to that channel. This suggests varying levels of crosstalk between different ports. Figures 10b
447 and 11b on the other hand show no measurable cross talk between any of the channels.

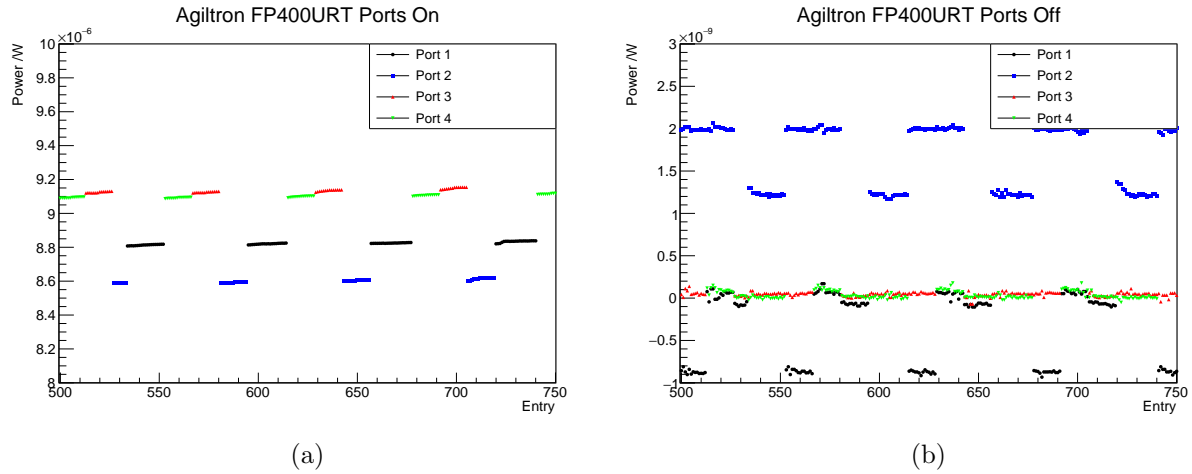


Figure 9: Power meter readings from all four ports for the Agiltron FP400URT device, zoomed into a shorter period of data to better show structure. Data is shown for when ports are a) illuminated and b) not illuminated. Note the different y-axis scales.

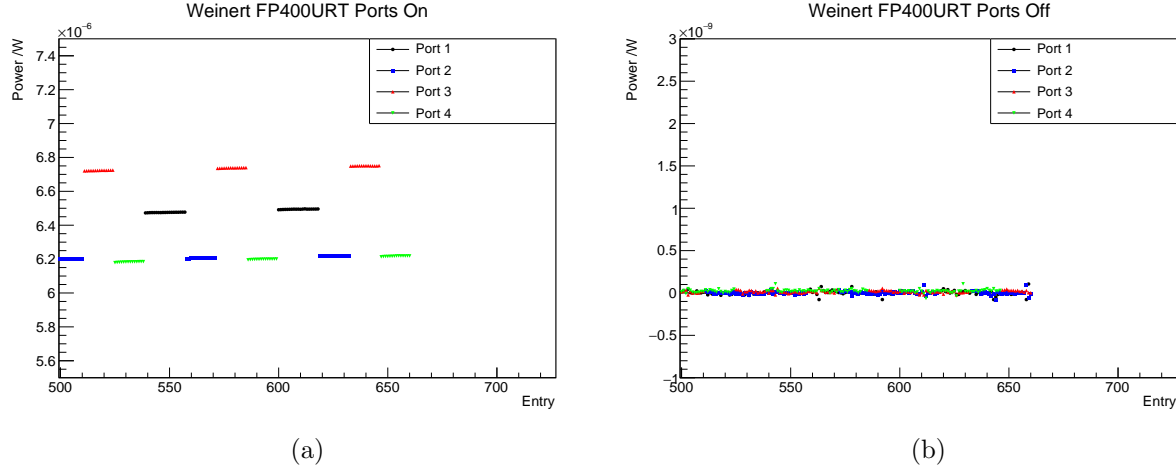


Figure 10: Power meter readings from all four ports for the Weinert FP400URT device, zoomed into a shorter period of data to better show structure. Data is shown for when ports are a) illuminated and b) not illuminated. Note the different y-axis scales.

448 To further investigate this, the way the data is plotted was inverted. The four plots in Figure 12
 449 show the power recorded on a specific port, each separated by which of the other three ports was
 450 illuminated at the time. While the absolute value of the power is not expected to be exactly zero
 451 due to global drift caused by temperature changes in the lab over the course of data taking, all four
 452 power meters were calibrated at the same time, so should show the same level of power when not
 453 illuminated. This is clearly not the case for ports 1 and 2 (Figures 12a and 12b), with the former
 454 showing higher power readings when port 2 or port 3 were illuminated, and the latter showing the
 455 same when port 3 or port 4 were illuminated. There is also a small offset observed for port 4 in
 456 Figure 12d, when port 3 is being illuminated. Interestingly, no obvious cross talk was observed to
 457 port 3, from any of the other ports being illuminated.

458 As no cross talk was observed for either of the Weinert devices, the corresponding plots are not
 459 shown here, but are given in Figures 27 and 28 in Appendix A for completeness.

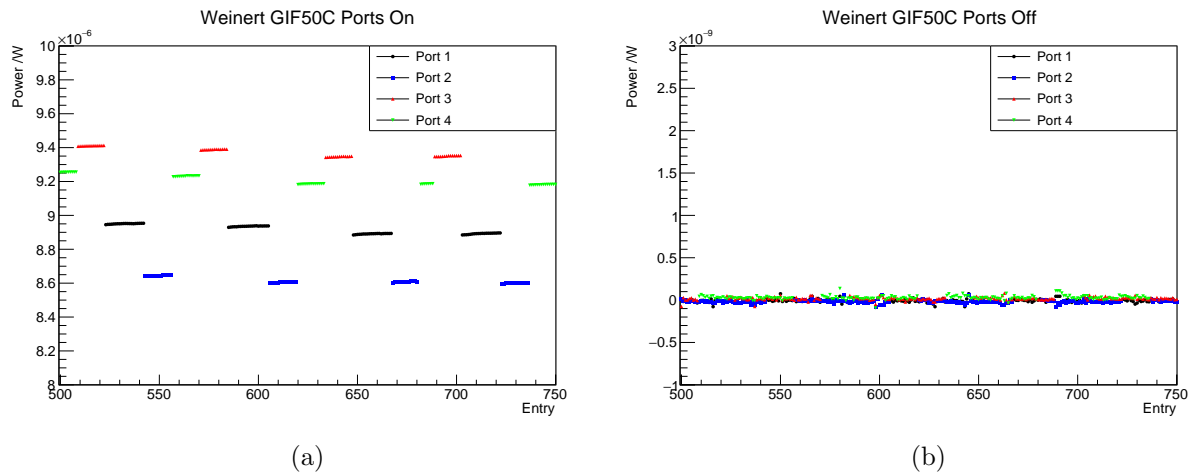


Figure 11: Power meter readings from all four ports for the Weinert GIF50C device, zoomed into a shorter period of data to better show structure. Data is shown for when ports are a) illuminated and b) not illuminated. Note the different y-axis scales.

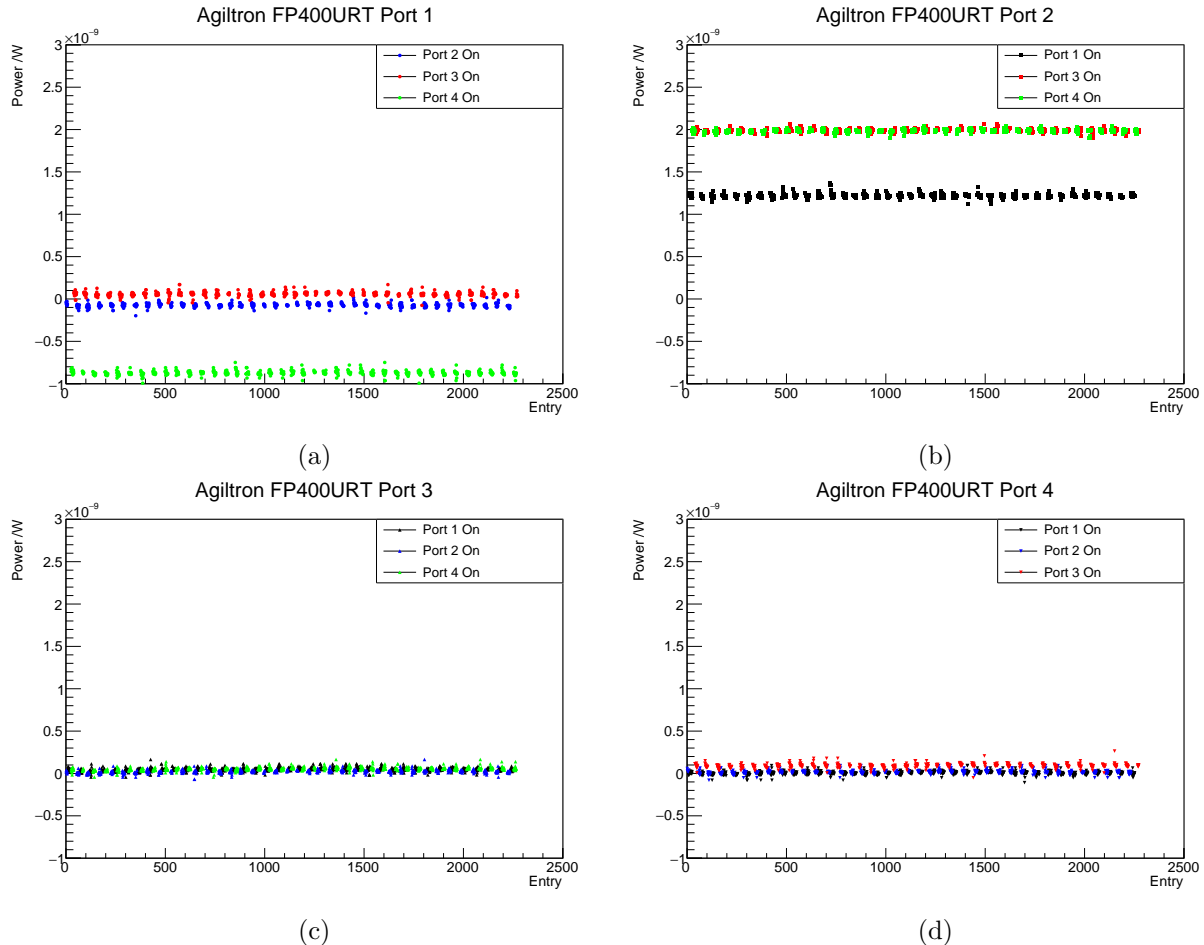


Figure 12: Power recorded on a) port 1, b) port 2, c) port 3 and d) port 4 of the Agiltron FP400URT switch, when one of the other three ports was illuminated.

460 5.4 Summary

461 Testing of the three different fibre switching devices finds different devices come out best based on
462 different factors. The Weinert GIF50C device showed best power transmission, with at most 4.7%
463 loss compared to the reference fibre, while the Weinert FP400URT device showed up to 27.6%
464 loss. This is with the caveat that the device package was different, and the latter had a greater
465 length of fibre than both the other devices and the reference fibre used. All devices exhibited under
466 5% variation in output power across the four ports, with the Agiltron switch showing the least
467 variation at a difference of 2.61%.

468 A clear preference for the Weinert devices comes from the cross talk measurements, which show
469 measurable cross talk between certain channels on the Agiltron device. While this is at the level
470 of $\mathcal{O}(0.1\%)$, the lack of any measurable cross talk from either of the Weinert devices is clearly
471 preferable. Coupled with the superior support from Weinert which will make setup and potential
472 servicing of the hardware easier, this is the device that is preferred. The internal fibre will of course
473 be chosen to match what is used for the rest of the laser system, so will be Thorlabs FG105UCA
474 or equivalent.

475 6 Speed of Light Measurements

476 As will be discussed in further detail in Section 9, the lengths of fibre optic cables connecting to
477 the injectors will not be uniform. This presents additional challenges for the system as different
478 path lengths result in different levels of attenuation and dispersion and, in particular, offsets in
479 delays between signals in the electronics and actual light injection into the tank. For example, the
480 injection event using a diffuser on the end of a ~ 160 m fibre will occur much later than when the
481 input light has to only traverse 10 m of fibre. To account for this, delays should be incorporated
482 into the electronics based on the expected time taken for a light pulse to be injected. To this end,
483 the speed of light within the FG105UCA fibre was measured, to understand if this offset could be
484 easily implemented.

485 Using the fibre test stand with the laser setup, the relative time delay between the laser trigger
486 signal and the PMT signal was recorded, for fibre lengths of 1 m, 35 m, 107 m and 142 m. As with
487 previous measurements, due to the fragility of the untubed 105 m reel of FP400URT, 1 m patch
488 fibres were used to connect it into the system. Time delay values were recorded at each length for
489 20,000 events, in order to obtain uncertainties. The results for this are shown in Figure 13, where
490 the data is fit with a linear function to calculate the necessary time delay in the electronics per
491 metre of fibre. This verifies that the speed of light can easily be measured with this setup, and
492 that including connectors has no obvious impact on the expected results. Naturally, as the speed
493 of light in any medium is wavelength dependent, this will need calculating for every wavelength of
494 light used in the LI system.

495 7 Destructive Testing

496 Another important aspect of the fibres to test is their durability. While every care should be taken
497 with the fibres to ensure damage does not occur, they will be installed in a working environment,
498 and accidents can happen. With a large number of fibres of varying length, visually noticing

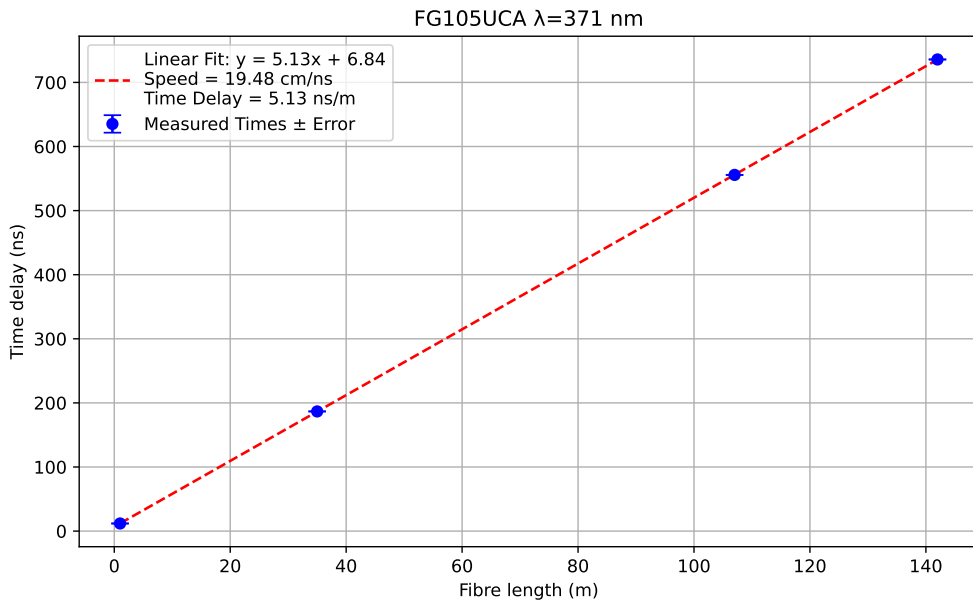


Figure 13: Time delay measurements from the FG105UCA fibres using the 371 nm laser head.

499 damage to a fibre is very unlikely. As such, it is important to understand what kinds of stress a
 500 fibre can realistically be exposed to and what can be tolerated, along with how to quickly check if
 501 damage has occurred.

502 As these tests need to be carried out in a working environment, using the same set-up as in the
 503 fibre optic test stand (Section 4.1) is not viable. Instead, commercially available, hand-held testing
 504 devices were investigated, and three units of the TREND Networks FiberMASTER MM testing
 505 kit [23] were purchased. This is a hand-held, battery operated light source and power meter, with
 506 varied wavelengths between 850–1550 nm. Although this is not the operating wavelength of the
 507 LI system, it still allows for quick checks of through-put power, and any damage to the fibres will
 508 still be obvious in changed readings.

509 A series of tests were carried out to assess the resilience of FP400URT and FG105UCA 1 m
 510 patch fibres to crushing, bending and cutting, plus scraping of the connector ends. The results for
 511 these are briefly summarised here. **can go into more detail if desired, but Unik has a lot**
 512 **of info that needs condensing into this section**

513 7.1 Crushing

514 The first set of tests carried out consisted of applying a series of increased weights to the fibres.
 515 This started with simply applying bodyweight (~ 80 kg) through stepping on the fibres, the most
 516 likely scenario for them to experience stress. No visible damage or change in power output was
 517 observed in this case.

518 To increase the force experienced, a trolley was used to apply a series of weights from 100–160 kg
 519 through a single wheel. At the maximum weight of 160 kg, a 24% reduction in output power was
 520 observed, but this returned to normal once the weight was removed. Visual inspection of the fibre
 521 revealed some yellowing caused by stress to the fibre, but no other signs of permanent damage
 522 were observed. To push this further, the fibre was then driven over by a small car (*sim* 330 kg per

523 wheel), while connected to the hand-held test kit. Static compression was seen to reduce the power
524 output by 60%, but again only while the weight remained on the fibre, returning back to nominal
525 after being removed. As a final test, the fibre was also exposed to shearing forces, by turning the
526 car's wheels whilst stationary on the fibre. This caused a sharp drop in power of 86% and clear
527 structural damage, as the power output did not recover after removing the weight.

528 7.2 Bending

529 These tests explored how the fibres responded to manual bending and twisting, particularly beyond
530 the specified bending radius. Fibres were observed to tolerate mild bends without degradation,
531 however when forming angles below 90° significant signs of degradation occurred, particularly if
532 bent in locations of previous wear. For the FG105UCA, a sharp bend in its midpoint caused a
533 power reduction of 35–55%, and ultimately breakage when folded back on itself. Results were
534 similar with the FP400URT. Though only exploratory, these tests highlighted the importance of
535 maintaining the quoted bending radius and the care that should be taken when deploying fibres.

536 7.3 Cutting

537 This test was to evaluate the physical resilience of the furcation tubing when exposed to sharp
538 tools. In these tests, a utility knife, pliers and scissors were used. The utility knife was unable to
539 penetrate the tubing with multiple passes, however the pliers and scissors were able to cut through
540 the whole fibre with moderate effort. This suggests that the furcation tubing is capable of holding
541 up to passing cuts, but not when blades are applied with reasonable force. Care should be taken
542 when working with any sharp object around fibres, and any exposure minimised.

543 7.4 Scraping

544 This test focussed completely on the fibre connectors, applying surface abrasion to simulate damage
545 caused by the connectors being dragged along floors or scraped against surfaces during installation.
546 Figure 14 shows microscope images taken of the connectors, where the extent of the damage to the
547 internal fibre core after scraping along the lab floor can easily be seen. A permanent reduction in
548 power of up to 50% was observed after causing this damage. This highlights the need to keep all
549 ends of fibres protected by dust caps throughout shipping, testing and installation, right up until
550 the point of connection.

551 8 Reception Testing

552 Section 9 will discuss the number of fibres required for the entire LI system to be built. In an ideal
553 scenario, all fibres will be delivered to Japan with no issues. However, with such a large order, the
554 potential for small defects in manufacturing or some damage in shipping must be accounted for.
555 A contingency of ~ 10% will be assumed in quotes to account for this. Upon receipt of the fibres
556 in Japan, several tests should be carried out to ensure the fibres are performing as expected.

557 With nearly 1000 fibres in total, full characterisation of each one is not viable. Instead, upon
558 delivery of each set of fibres, quick checks of power output through each fibre will be performed with
559 the hand-held testing device detailed in Section 7. By measuring the transmitted power through



Figure 14: Microscope images of connectors for FP400URT (left) and FG105UCA (right) before (top) and after (bottom) scraping along the lab floor.

560 all fibres in a set a distribution of values can be built, and the largest outliers excluded down to
 561 the number of required fibres. Specification sheets for the FG105UCA [10] and FP400URT [8]
 562 provide measured attenuation values for a range of wavelengths. By comparing the batch average
 563 power to the expectation when accounting for attenuation, any difference should be immediately
 564 obvious, and significant issues would be raised with the supplier straight away. During installation
 565 of the fibres, power readings with the hand-held devices will be repeated, to ensure no damage has
 566 occurred to fibres in the process.

567 While it will not be possible to extensively test all fibres, more detailed batch testing of fibres
 568 upon delivery to Japan is required. This will be carried out using a very similar set-up to the
 569 Liverpool fibre optic test stand (described in Section 4.1), which will be reproduced in the lab
 570 space in Japan, using the laser system which will then be installed as a light source for the ID
 571 injectors. Arguably the most important measurements to be made here will be those of the speed
 572 of light in fibres. These will be carried out following the same prescription as in Section 6, for
 573 both fibre types. As the speed of light in a medium is wavelength-dependent, this will be done for
 574 every appropriate wavelength, with the measurements being used to define the required offsets in
 575 electronics to account for different lengths of fibres used. In addition to speed of light measurements,
 576 batch testing of attenuation and pulse widths will be carried out to screen for potential issues.

577 9 Fibre Length Requirements

578 With the large number of injectors being employed for the light injection system, an even larger
 579 number of fibre optic cables will be required. This section details the quantity and lengths of cables
 580 required to connect the full HK LI system.

581 The overall design of the HK water tank and PMT support structure is given in Figure 15.
 582 Fibre optics will run through specifically installed fibre ports around the edge of the dome floor into

the OD, then down to each injector location. 16 of these fibre ports are distributed roughly evenly

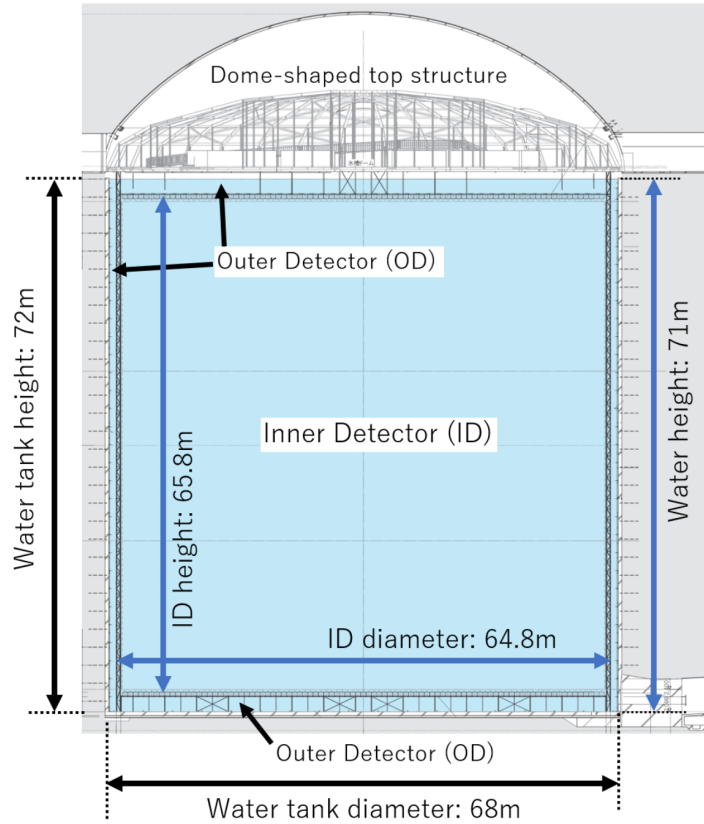


Figure 15: Schematic of the HK water tank and PMT support structure.
[24]

583
584 around the outer edge of the dome. The full schematic of the dome showing all calibration and
585 fibre ports is given in Figure 16. The OD fibre ports in question are those marked with magenta
586 dots and labelled “odf” (OD(ニアイバー用)).

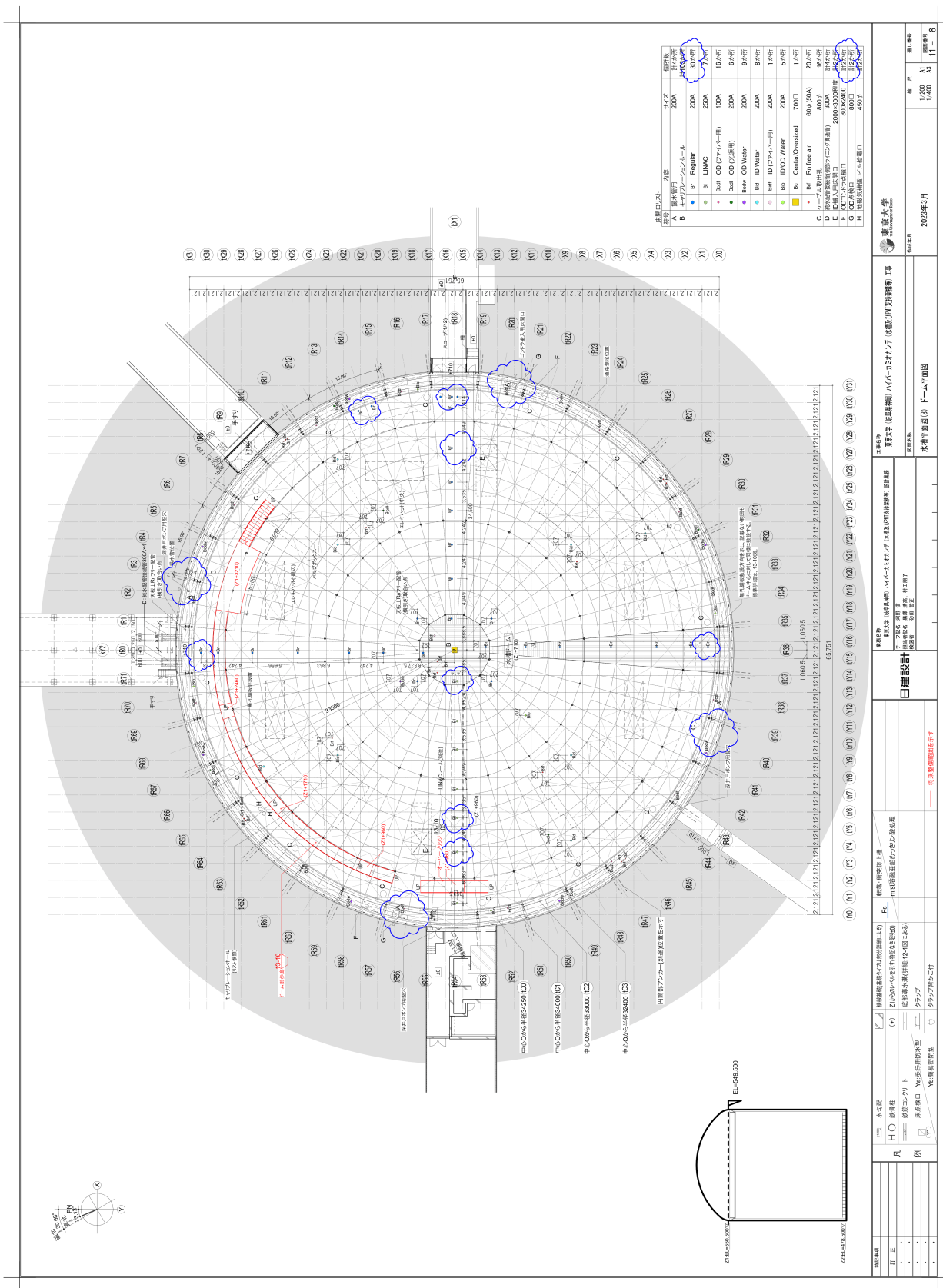


Figure 16: Top down view of the HK experimental area on top of the tank, showing locations of various calibration and fibre ports.

587 In order to limit the effect of potential damage to fibres, these will be split into in-tank and
588 out-of-tank fibres. The fibres laid along the top deck will run from the calibration rack near the
589 centre of the dome to patch panels next to the OD fibre ports. Being on the deck where there will
590 be foot traffic for up to 20 years, the out-of-tank fibres are most likely to get damaged. Keeping
591 them separate to the in-tank fibres makes replacing damaged fibres much easier, as it would be
592 implausible to replace the in-tank fibres.

593 The initial preference for the fibre layout was to keep all fibre lengths the same. While this
594 would involve many injectors being attached to fibres that were unnecessarily long, it would mean
595 that the attenuation, dispersion and timing delays of pulses sent to all injectors would be constant.
596 However, during the process of obtaining quotes, it was discovered that manufacturing a large
597 number of fibres over 100 m would be problematic for the FP400URT, as draw lengths above
598 100 m are rare. This is problematic as lengths of \sim 120 m are required to reach from the OD fibre
599 ports to the centre of the bottom end-cap. To work around this, in-tank fibres will be split into
600 two parts, one extending to the bottom of the barrel, and another extending across the bottom
601 end-cap. Connectors will be installed on the bottom corners of the tank to facilitate this.

602 With multiple in-tank fibres needing to be connected together to reach the injectors on the
603 bottom end-cap, it no longer makes sense to make all injector path lengths the same. Therefore,
604 the required lengths need to be calculated for each section, based on deployment method and path
605 taken.

606 9.1 Injector Cell Locations

607 9.1.1 Barrel Injectors

608 As shown in Figure 1, the ideal ID injector layout features seven injector layers in the ID, equally
609 separated. In reality, injector locations will be constrained by the available cells not already
610 occupied by the PMTs, cable drums or various kinds of electronics vessels within the PMT support
611 structure. Figure 17 shows an example of this, for the bottom 12 cells of a 30° section of the
612 barrel PMT support structure. There will be a total of 92 cells in the vertical direction. During
613 construction, the barrel PMT support frame will be constructed in layers of four cells at a time.
614 Once the full layer is complete and the respective components installed, the layer will be raised, and
615 the next four cells constructed underneath. During construction of each four-cell layer, scaffolding
616 will be required to work on the top two cells. To avoid this, installing injectors in the bottom
617 two cells of each four-cell layer is planned. As the bottom cell of each layer is often dominated
618 by electronics vessels, the second cell is preferable for injector locations. Dividing the total height
619 into eight parts and taking the closest second layer yields the vertical cells given in Table V. This
620 results in a set of seven vertical cells symmetrical around cell 46, the top of which is at the centre
621 of the tank. Table V also lists the z position of the bottom of the cell, using cell heights of 707 mm
622 and again treating the top of cell 46 as $z = 0$ mm. To get the injector z coordinates an offset
623 is added to each, accounting for the 125 mm width of the horizontal bars, and then assuming an
624 extra 50 mm to account for diffuser mounting and radius.

625 To define the horizontal location of cells, the radial labelling of the vertical support struts
626 shown in Figure 16 is used, starting from tR0 and running to tR71 in the clockwise direction.
627 Between each of these supports is a 5° angle, containing four cells. As no standard cell labelling

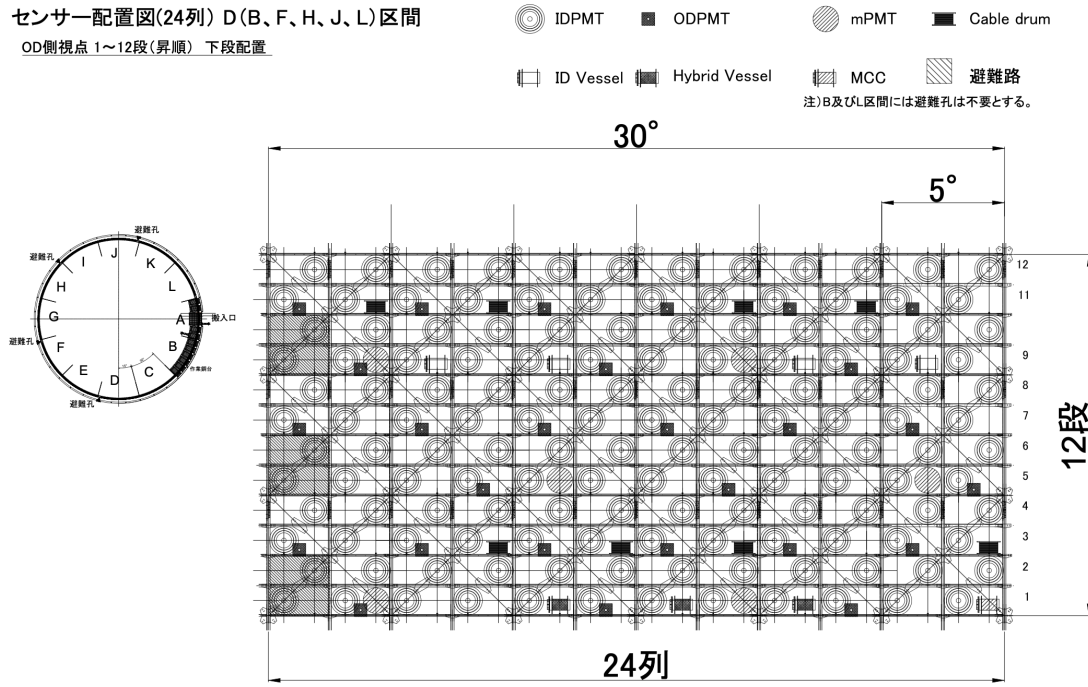


Figure 17: Diagram showing cells 1-12 of a 30° section of the barrel PMT support structure, with fixed locations of components marked, as seen from the OD side of the structure.

ID vertical label	Vertical cell	Cell z position (mm)	Injector z position (mm)
1	82	24745	24857.5
2	70	16261	16373.5
3	58	7777	7889.5
4	46	-707	-594.5
5	34	-9191	-9078.5
6	22	-17675	-17562.5
7	10	-26159	-26056.5

Table V: Vertical cell locations for both ID and OD barrel injectors. Cell z position is defined as the bottom of the cell, and injector position assumes the injector being installed at the bottom of the cell, accounting for the width of horizontal bars and radius of injectors.

628 currently exists in the horizontal, we label each cell 1 through 4, again in the clockwise direction,
 629 resulting in a horizontal cell label of the form $tR X.Y$, where $X \in \{0..71\}$ and $Y \in \{1..4\}$. As
 630 Figure 17 is viewed from the OD side, vertical support labels and cell numbers increase from right
 631 to left. **These cell addresses will be updated once a common system is decided within**
 632 **the integration group.**

633 As one column of ID injectors will coincide with the position of the Korean LI system, the
 634 horizontal positions are dictated by this. The Korean LI system will be installed between the two
 635 regular calibration ports (labelled ‘Br’ in Figure 17) either side of tR14. Based on the previous
 636 requirements for cell choice, tR13.4 is the optimal choice for injector placement in this region, for
 637 the Korean LI and the ID LI optics. Placing LI ID injectors at every 90° this sets the remaining
 638 horizontal cell locations as tR31.4, tR49.4 and tR67.4.

The OD diffuser ideal positions are shown in Figure 2, where again there are seven vertical positions within the barrel. To simplify installation, the vertical positions for the ID and OD diffusers in the barrel will be aligned. As each layer of OD barrel diffusers is offset from the previous by 15° , this results in OD diffusers in the same cells as ID injectors for only layers 1, 3, 5 and 7. Starting from the overlap cells, and placing 12 diffusers in each layer (one every 30°), results in the OD diffuser barrel cell locations listed in Table VI.

Vertical label	1, 3, 5, 7	2, 4, 6
Horizontal cell	tR1.4	tR4.4
	tR7.4	tR10.4
	tR13.4	tR16.4
	tR19.4	tR22.4
	tR25.4	tR28.4
	tR31.4	tR34.4
	tR37.4	tR40.4
	tR43.4	tR46.4
	tR49.4	tR52.4
	tR55.4	tR58.4
	tR61.4	tR64.4
	tR67.4	tR70.4

Table VI: Cell locations for OD barrel diffusers.

While the exact positions of the 12 OD collimators are yet to be set, the rough locations for mounting have been decided. Three will be installed on the edge of the top end-cap, while the other nine will be installed on the edge of the bottom end-cap.

9.1.2 End-cap Injectors

For the ID injectors, the top-end cap will have a single location. The diffuser and collimator will be installed through the ID fibre port, labelled ‘Bidf’ in Figure 16. Only one position here is needed, as the injectors can easily be removed in the case of any faults. For the bottom end-cap this is of course not possible, and so four sets of injectors will be installed around the centre for degeneracy. A diagram of an end-cap is shown in Figure 18. The locations of PMTs and electronics vessels shown will be the same for both top and bottom. Only the ports (shown in yellow) are unique to the top end-cap.

For the OD, 19 diffusers will be installed on each end-cap. The locations of these, which are again same for top and bottom, are shown in Figure 18, denoted by cyan stars. These positions are chosen to match as closely as possible to the ‘ideal’ layout shown in Figure 2. **Exact cell locations will be provided once a cell address scheme is decided upon by integration group.**

9.2 Fibre Paths

With the locations of the injectors decided, the routes of fibre optic cables to said injectors can be planned, and the required lengths of each set of fibres obtained. Installation of the majority of fibres will take place after construction of the PMT support structure is completed. A small

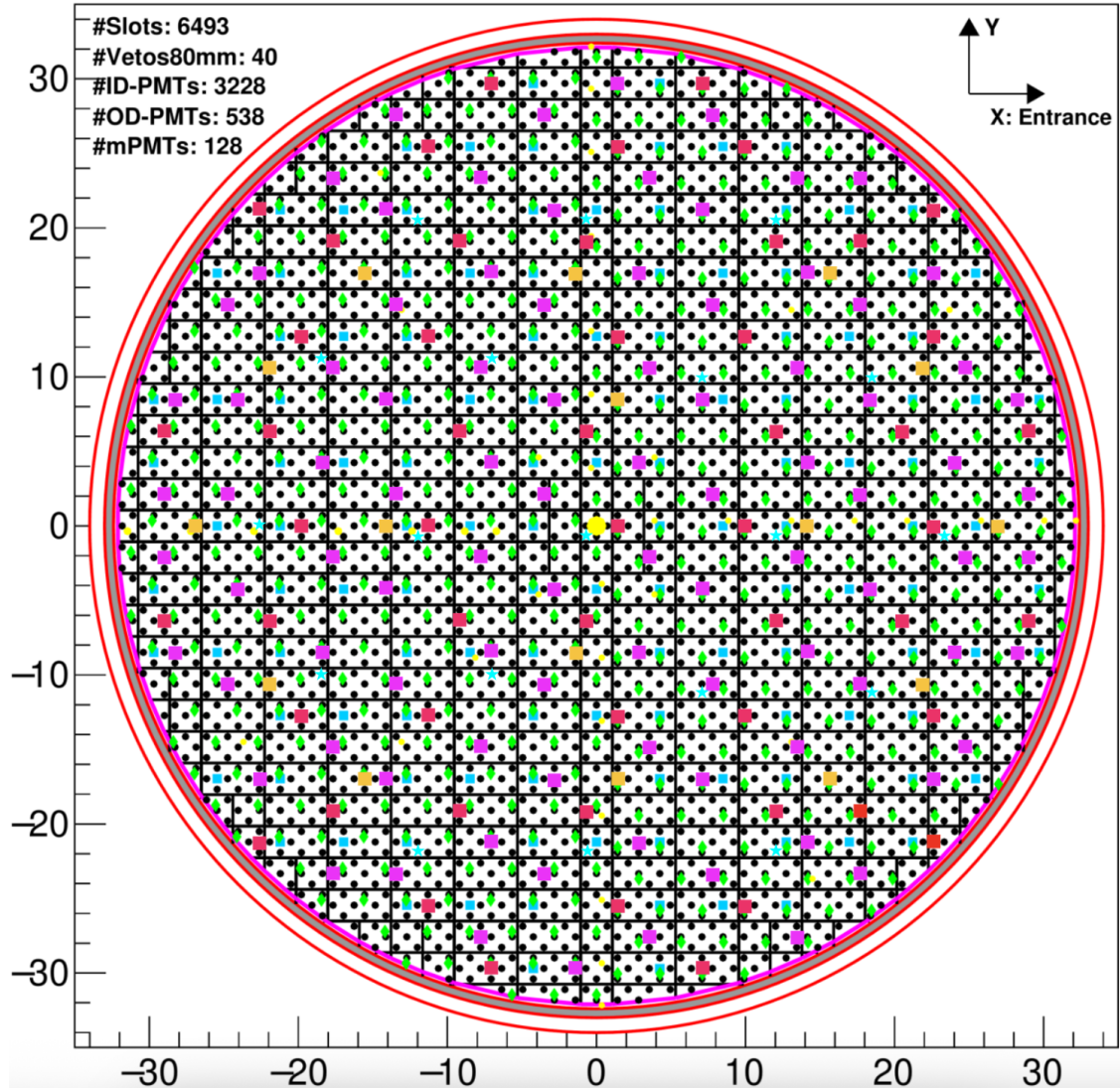


Figure 18: Diagram of PMT support structure end-cap, with a variety of components' locations shown. Other than calibration ports (yellow circles), mapping is the same for both top and bottom end-caps. The location of OD diffusers is shown with cyan stars.

team of experts will enter the tank in the OD gondola, using this to route fibres around the tank. Given the size of the Hyper-K tank, and the low speed of a gondola (initial designs estimate this at 0.2 ms^{-1}), many decisions made here are in an effort to make installation as efficient as possible.

9.2.1 Top Deck

This set of fibres is used to run from the calibration racks near the centre of the top deck, to respective OD calibration ports around the edge, where they will attach to patch panels. This will be done for all injectors except for the top ID injectors, and top OD diffusers. The preferred method for installation is for the fibres to be laid into cable trays underneath the deck, to limit the chance of breakage from exposure to foot traffic. In mapping these routes out it is assumed that the fibre can travel in a straight line from rack to port, with the exception of having to avoid any structures that penetrate the deck to the tank, such as ports and gondola hatches. The proposed routing is shown in Figure 19, though the exact location within the calibration area marked in blue

that the fibres would meet is as yet unknown. The only fibres which cannot travel in a straight line are those to ODF5 and ODF13, as they have to bend around the marked ID gondola hatches. Using this as a guide, the required fibre lengths can be calculated. As the point that the fibres will exit at the calibration rack is unknown, the unit 2121×2121 mm square is highlighted, and the distance to the closest edge of this measured. To account for the unknown distance within the square, and any vertical travel required up the calibration rack, an addition of 5 m will then be applied to every required length. The actual measurement of each fibre is done by the pixel

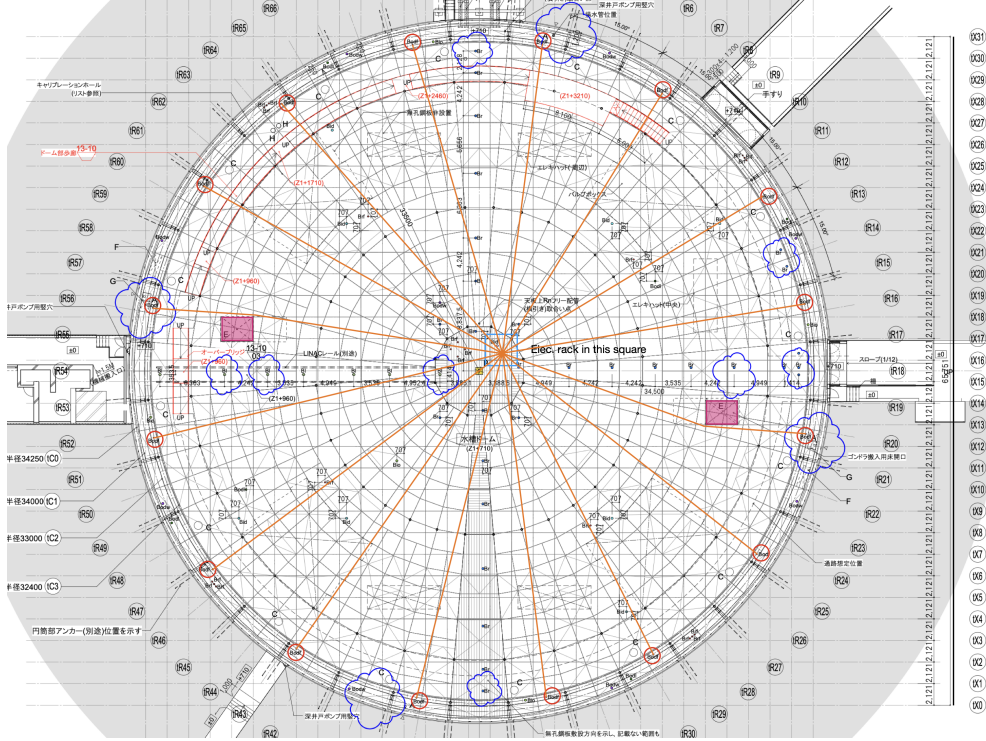


Figure 19: Diagram of fibre routing below deck from calibration rack to OD fibre ports. OD ports are circled in red, ID gondola hatches outlined in purple, and the blue square shows a $\sim 3 \times 3$ m square where the calibration racks will be. Orange lines show the proposed fibre routes.

length of each line from rack to port. The total diameter of the tank is measured to be 984 pt. As this is shown in Figure 20 to be 65751 mm, this equates to 1 pt = 66.82 mm \simeq 67 mm. Using this, the required length of each fibre can be calculated. These values are summarised in Table VII.

The maximum length requirement found here is 34572 mm, to get to ODF 11. Adding the 5 m to account for reaching the calibration rack and travelling vertically to the specific crate gives a total distance of 39572 mm. This can then be rounded to 42 m for safety, and to ensure the fibres have some slack in them. As both ends of the fibres will connect to patch panels, each end of the fibre should have an FC/PC connector, for both fibre types.

9.2.2 Barrel Fibres

There are two sets of fibres which need to run down the side of the barrel: those that connect to barrel injectors, and those that must run to the bottom of the tank to reach bottom end-cap

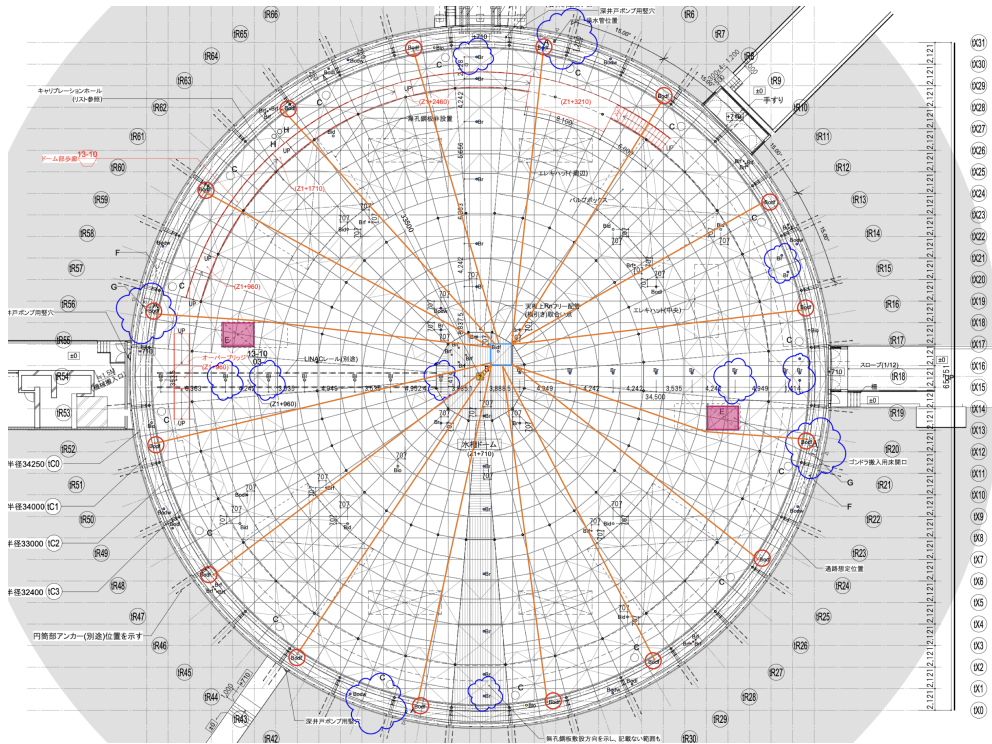


Figure 20: Same as Figure 19, except the blue square outlines the $\sim 2 \times 2$ m square within which the fibres could potentially exit the deck, as the exact location of the calibration rack is not known. In this case the orange lines are used to measure distance from respective calibration port to the edge blue square. This is not the map used for fibre routing itself.

696 injectors. As these will both take the same paths down the vertical supports, they are included
697 together here.

698 To route these fibres to either a barrel injector or bottom end-cap, the fibres will run through
699 one of the 16 OD calibration ports. These ports extend 1200 mm below the top of the tank, into the
700 dead region of the PMT support structure. At the point where the fibres exit the port, they will be
701 routed to one of the two neighbouring vertical supports. The support chosen will not necessarily
702 be the closest one, as choices should be optimised for efficient installation. The mapping between
703 horizontal cell location, fibre port, and vertical support to route down is shown in the first three
704 columns of Table VIII. As should be clear from this, the majority of injectors will not have the
705 fibre run directly down to them. Instead, each fibre will run down the respective vertical support
706 until at the same horizontal level as the injector, before being running radially around the side of
707 the detector to reach the injector cell. In both ID and OD cases this will be done on the outer edge
708 of the support structure; for OD diffusers this is where they will be housed. For the ID injectors,
709 a patch cable to span the dead region will have been installed at the same time as the injector
710 housing itself, to avoid the person connecting the fibre having to reach out of the gondola into the
711 dead region.

712 To calculate the maximum amount of additional fibre needed to account for this horizontal
713 travel, the angular difference between each injector cell and the respective vertical support used to
714 route down can be calculated. This is done assuming the injector is installed in the centre of a cell,
715 with the values given in the final column of Table VIII. Taking the maximum angular difference of

Port ODF no.	Length [pt]	Length [mm]	Port ODF no.	Length [pt]	Length [mm]
1	437	29279	9	512	34304
2	426	28542	10	515	34505
3	427	28609	11	516	34572
4	437	29279	12	513	34371
5	$152 + 301 = 453$	30351	13	$153 + 349 = 502$	33634
6	465	31155	14	481	32227
7	489	32763	15	468	31356
8	503	33701	16	451	30217

Table VII: Required length of fibre to reach from each OD fibre port to the 2121×2121 mm square the calibration rack is assumed to be in.

716 10.625°, an arc length of 6130 mm is found. The same has to be done for the distance between the
 717 OD fibre port and the vertical support. As the locations of the ports are not precisely documented,
 718 the maximum angular distance of 5° is taken, equating to 2885 mm. These additions will apply
 719 to all barrel injectors. For the fibres needed to reach the bottom, only the horizontal addition for
 720 port to vertical distance is required.

721 Vertical and total length requirements for the barrel fibres are easily found from the vertical
 722 cell locations given in Table V, using a cell height of 707 mm, and a distance from the deck to top
 723 of cell 92 of 3935 mm. This again uses a bar width of 125 mm, and assumes a 50 mm offset to
 724 account for the height of the injector. The calculated values are shown Table IX. These numbers
 725 show that the additional horizontal fibre required to reach from vertical supports to an injector cell
 726 is not a problem, as the maximum length case still comes from reaching to the bottom of the barrel.
 727 For contingency, and to allow fibres to not be kept taught, the maximum length requirement is
 728 rounded up to 76 m. For the ID system, all fibres will have FC/PC connectors on either end. This
 729 is the same for the OD system fibres which traverse the entire barrel depth to the bottom end-cap.
 730 For the fibres connecting to OD barrel diffusers however, these will be polished fibre on one end,
 731 as this is what has to be pushed into the back of the diffuser hemisphere.

732 The plans presented here are used to calculate the maximum required length. Rather than have
 733 all fibres that traverse the barrel the same length, an alternative option is to split into three sets
 734 of fibres so that the amount of excess fibre can be limited, particularly for the higher up injectors.
 735 In this case, there is one length for vertical labels 1 and 2, one for 3, 4 and 5, and one for 6, 7,
 736 and fibres to the bottom of the barrel. The lengths of these are calculated using the values from
 737 Table IX, and are given in Table X. From both a cost and installation perspective, this case using
 738 three different lengths of fibre for the barrel injectors is the preferred method.

739 As mentioned in Section 9.1.1, there will also be 12 OD collimators affixed to the barrel/end-
 740 cap edges; three on the top and nine on the bottom. The bottom collimators will require the
 741 aforementioned amount of fibre needed to reach the edge of the bottom end-cap. For the top ones,
 742 which will also be connected through the OD fibre ports, a length of 10 m will be enough to connect
 743 these.

Inj. cell	ODF	Vertical to route down	Port to inj. angle [°]
tR1.4	1	2	0.625
tR4.4	2	6	5.625
tR7.4	2	6	9.375
tR10.4	3	12	5.625
tR13.4	4	15	5.625
tR16.4	4	15	9.375
tR19.4	5	20	0.625
tR22.4	6	25	10.625
tR25.4	6	25	4.375
tR28.4	7	29	0.625
tR31.4	8	33	5.625
tR34.4	8	33	9.375
tR37.4	9	38	0.625
tR40.4	10	43	10.625
tR43.4	10	43	4.375
tR46.4	11	47	0.625
tR49.4	12	52	10.625
tR52.4	12	52	4.375
tR55.4	13	57	5.625
tR58.4	13	57	9.375
tR61.4	14	61	4.375
tR64.4	15	65	0.625
tR67.4	16	70	10.625
tR70.4	16	70	4.375

Table VIII: List of all barrel injector horizontal cell locations, with corresponding OD fibre port to route through, vertical support to route down, and angle between the given vertical support and the injector cell. This assumes injector installation in centre of cell.

Vertical label	Layer	Vertical dist. from deck [mm]	Total dist. from port [mm]
1	82	11617.5	20632.5
2	70	20101.5	29116.5
3	58	28585.5	37600.5
4	46	37069.5	46084.5
5	34	45553.5	54568.5
6	22	54037.5	63052.5
7	10	62521.5	71536.5
Bottom	0	70412.5	73297.5

Table IX: Vertical and total travel distance to reach to a given layer of barrel injectors. Both distances are calculated from the deck, but the total distance takes into account maximum required travel from port to vertical and vertical to injector. Only the port to vertical distance is added for fibres extending to the bottom end-cap.

Region	Length [m]
1+2	32
3+4+5	58
6+7+bottom	76

Table X: Total length requirements for barrel fibres, in the case where lengths are split for different barrel regions to reduce excess fibre.

9.2.3 Bottom end-cap

To reach the injectors on the bottom end-cap, a final set of fibres is required. These will run from the connectors installed on the bottom edge of the PMT support structure, to a given injector position. In order to simplify installation, the bottom end-cap cable mapping is optimised to only run from four vertical supports, minimising the number of times the gondola will need to traverse the full height of the tank. In doing this ODF4 is also avoided, as this is the port that the Korean injector fibres will also run through, and it is preferable to not overload a single port or vertical support with fibres. The proposed fibre routing map for the bottom end-cap OD diffusers is shown in Figure 21. This involves having connectors at the bottom of verticals tR12, 33, 52 and 65, and thus will utilise ports ODF 3, 8, 12 and 16 for the barrel segments of these fibres, respectively. From the connector, the end-cap portion of the fibre will be routed to the ID side of the support structure, at the closest point where the orthogonal bars shown in Figure 21 meet it. The fibres must then follow this orthogonal path to reach the injectors. Required fibre lengths are measured simply by counting the unit lengths they must traverse, where the 3×3 cell size defines $1u = 2121$ mm. These lengths are given in Table XI for each OD end-cap bottom (ODEB) diffuser. As would be expected, the greatest length of fibre is needed to reach the diffuser position in the centre, ODEB10. This needs a distance of $18u = 38178$ mm. In order to simplify things, this is rounded to 42 m, matching the lengths needed for the deck fibres described in Section 9.2.1. All of these OD diffuser fibres will need to have an FC/PC connector on one end, and polished bare fibre on the other.

Not shown here are the ID injector positions. Each of the four sets will be positioned in one of the four 3×3 cell squares diagonally adjacent to the central square. The longest fibre for these is

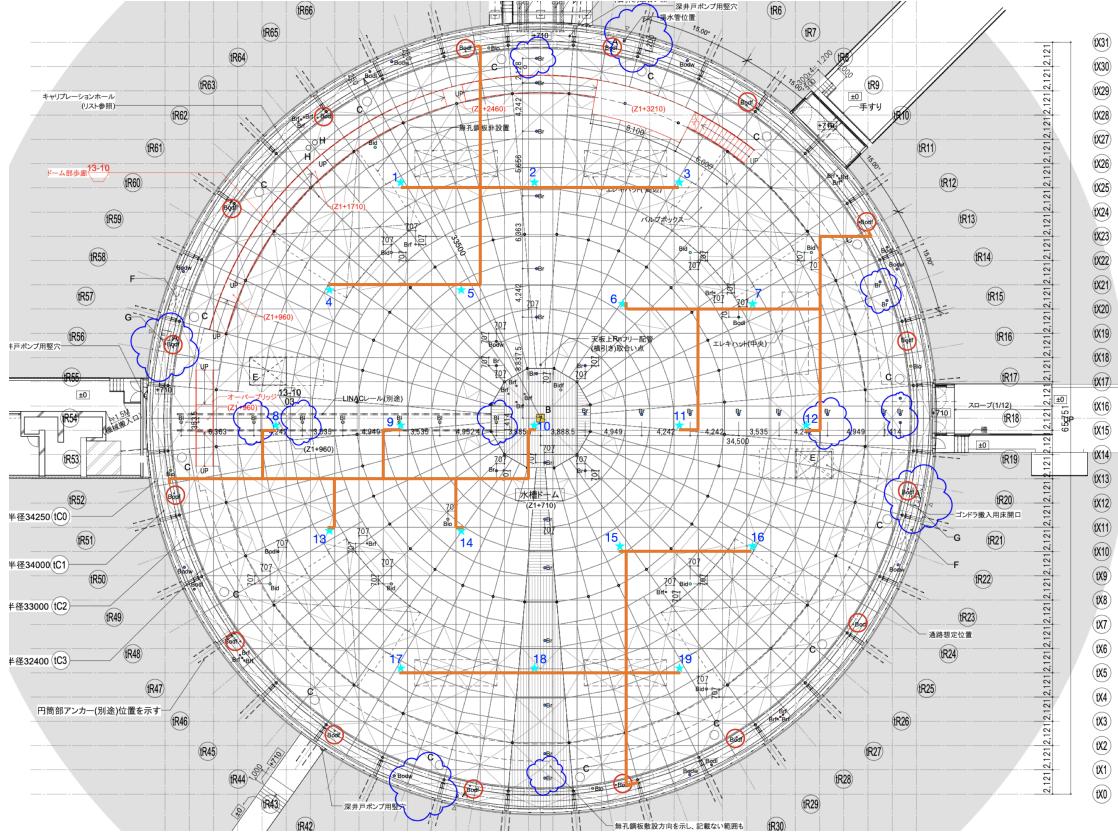


Figure 21: Map of OD diffuser positions on end-cap (cyan stars), showing fibre routing plan specifically for the bottom end-cap. Schematic shown is for the deck so port positions do not apply, but diffuser positions are the same on top and bottom.

ODEB	Vertical	Distance [u]	ODEB	Vertical	Distance [u]
1	65	10	11	12	17
2	65	9	12	12	12
3	65	15	13	52	10
4	65	17	14	52	15
5	65	11	15	33	12
6	12	15	16	33	17
7	12	9	17	33	16
8	52	8	18	33	10
9	52	13	19	33	9
10	52	18			

Table XI: Required distance of fibre optic cable to reach each OD end-cap bottom (ODEB) diffuser, in units of 2121 mm. Also shown is the vertical support that the fibre will be routed from the bottom of.

766 required to run from vertical tR33 to the top right injector, measuring a length of $19u = 40299$ mm.
 767 This is still below the decided 42 m length, so causes no issues. **Exact cell location will be**
 768 **updated once we have a decided system.** These fibres will require FC/PC connectors on both
 769 ends.

9.2.4 Top end-cap

As previously mentioned, the ID injectors for the top end-cap will be deployed through the Bidf calibration port, meaning that they can be easily removed and replaced should the need arise. In this case, only one section of fibre is needed to go from the injectors to the calibration rack. The length of these is chosen as 10 m, well above the 4506 mm height of the described port. Both ends of these fibres will require FC/PC connectors on. This also matches to the length chosen for the top OD collimators.

The OD diffusers on the top end-cap (labelled ODET 1–19) will be installed in exactly the same x and y locations as for the bottom end-cap. The difference is in the fibre routing, as there is no easy way to get the fibres from an OD fibre port back up to the top end-cap frame. Instead, all of these fibres will also be routed through the Bidf calibration port, and then spread out from this position to each respective diffuser. The fibre routing map for this is given in Figure 22. In a

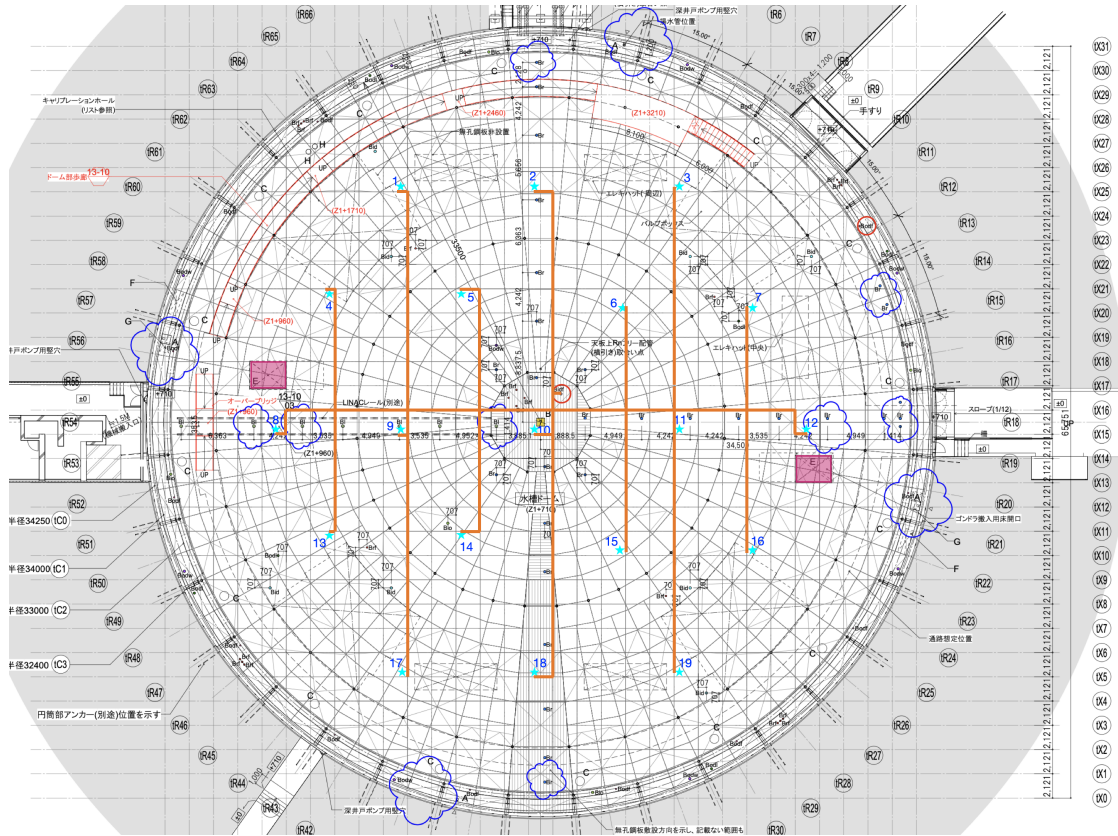


Figure 22: Map of OD diffuser positions on end-cap (cyan stars), showing fibre routing plan specifically for the top end-cap. All fibres will be deployed through the Bidf calibration port.

similar way to Section 9.2.3, the required lengths for these fibres are measured simply by counting the unit lengths along each path. The fibre lengths needed for each injector are given in Table XII. The greatest length of fibre required comes from connecting to ODET17, the furthest injector from the calibration port. This requires 19 units of length, equating to 40299 mm. Adding on 4506 mm for the height of the calibration port, and then 3000 mm for travel to the electronics rack, a maximum requirement of 47805 mm is obtained. The length of these fibres is therefore rounded to 50 m for contingency. As with the other fibres connecting directly to the OD diffusers, these will need to have FC/PC connectors on one end, and a polished bare fibre on the other. It should

ODET	Distance [u]	ODEB	Distance [u]
1	18	11	8
2	10	12	14
3	17	13	17
4	17	14	11
5	11	15	11
6	10	16	16
7	15	17	19
8	15	18	14
9	10	19	18
10	4		

Table XII: Required distance of fibre optic cable to reach each OD end-cap top (ODET) diffuser, in units of 2121 mm.

790 be noted that installation of injectors and fibres on the top end-cap is planned to be carried out by
 791 company workers rather than researchers, due to additional complications foreseen in this work.

792 9.2.5 Patch Fibres

793 Along with the long lengths of fibres described in the previous sections, a large number of patch
 794 fibres will be required at various points within laser and LED systems.

795 As described in Section 9.2.2, to connect to all ID injectors bar the top end-cap ones an ad-
 796 dditional patch fibre is also required. ID injectors will be installed on the PMT support structure
 797 during construction, while the fibre installation will be carried out after construction of the struc-
 798 ture has been completed, by utilising the OD gondola. In order to avoid workers having to reach
 799 far out of the gondola, through the support structure, to attach fibres to the injector housing,
 800 short patch fibres will be attached to the injectors at the time of their installation. These will
 801 span the dead region and be fixed to the outer side of the structure, so that the long fibres can be
 802 connected directly to the patch fibres. As part of this a fibre guide will be used, to ensure that the
 803 end of the fibre will be pointing vertically upwards for connection, without the fibre being pushed
 804 past its bending radius. The required lengths have been measured using a mockup of the support,
 805 obtaining values of 640 mm for the diffuser and 530 mm for the collimator. Both ends of these
 806 patch fibres will need to have FC/PC connectors.

807 Based on Figure 3, eight patch fibres will be required for within the laser system itself, not
 808 including the five that will come coupled to the laser heads. Five of these will run from individual
 809 attenuators to connect the laser heads to the 1x8 switch, and then three are used for the connections
 810 between the 1x8 and 1x80 switch, which includes integrating the fibre splitter for the monitor PMT.
 811 These will all be FG105UCA fibres with FC/PC connectors on either end, with a rough length
 812 requirement of ~50-~100 cm.

813 A series of short patch fibres will also be required for the LED system. Each LED pulser board
 814 will feature a connector sitting atop the surface mounted LED, with space for two fibres to be
 815 inserted. One of these will be directly above the LED to collect as much light as possible, and
 816 this will be used for illuminating the OD diffusers. The second will be offset, collecting some of
 817 the remaining light to be used as a signal for monitoring purposes. As the monitor system will
 818 sit at the electronics rack, much less fibre will be used and therefore less initial light input is

819 required. The design for the the fibre connector is currently ongoing, and will be used to confirm
 820 the required length of the patch fibres within the pulser board crates. Initial measurements of the
 821 required lengths, which are different due to the topology of the connector, give 21.1 ± 1.4 cm and
 822 18.4 ± 0.6 cm, where the uncertainties here are the measured tolerances on the length. Any shorter
 823 than this and the cable will not reach. If the cables are longer, they would be required to bend at
 824 a greater angle than their specified bending radius, which will cause degradation over the lifetime
 825 of the system. As the connector for the LED pulser board will have the fibres epoxied in, each of
 826 these patch cables will require FC/PC connectors on one end, with the other cleaved and polished.

827 The final set of patch cables for the LED pulser system is that used to connect to the monitor
 828 PMTs. The internal patch cable from the LED connector will go into a patch panel on the front
 829 of the electronics rack. These patch cables will carry light from that patch panel to a system
 830 of several monitor PMTs in the same electronics rack. These will be 1 m long, with an FC/PC
 831 connector on the patch panel end, and polished bare fibre at the PMT-facing end.

832 Tables XIII and XIV summarise all the required fibres for the laser and LED systems respec-
 833 tively, detailing the chosen type, length, connectors and quantities needed. Quantities are also
 834 detailed for the cases where the fibres that traverse the barrel region are split into different lengths
 835 to minimise excess, which is the preferred approach for this system. In these tables, fibres of the
836 same configuration are grouped together. Tables XVI and XVII in Appendix B breaks this down
837 further for additional clarity. As discussed in Section 4.3.2, all fibres will be tubed using the
838 Thorlabs FT030-BK tubing, the same as used for the UKLI system in Super-K. The exception to
839 this is the LED crate fibres, which will instead be colour-coded.

Length [m]	Connector A	Connector B	Required no.	Use
76	FC/PC	FC/PC	73	Barrel (all) [†]
42	FC/PC	FC/PC	84	Deck and bottom
10	FC/PC	FC/PC	5	Top ID inj. and top OD coll.
0.64 ¹	FC/PC	FC/PC	32 ⁸	ID-diffuser <u>Laser system</u> patch cable
0.56 ^{0.64}	FC/PC	FC/PC	32	ID collimator <u>diffuser</u> patch cable
0.5 ^{0.56}	FC/PC	FC/PC	8 ³²	Laser system <u>ID collimator</u> patch cable

[†] Staged approach:				
32	FC/PC	FC/PC	16	Barrel (levels 1+2)
58	FC/PC	FC/PC	24	Barrel (levels 3+4+5)
76	FC/PC	FC/PC	33	Barrel (levels 5+6+7 ⁷ +bottom)

Table XIII: List of all required fibres for the laser system with necessary lengths, connector configurations, quantities and uses.

Length [m]	Connector A	Connector B	Required no.	Use
76	FC/PC	FC/PC	19	Barrel to bottom
76	FC/PC	Bare	84	Barrel injs (all) [†]
50	FC/PC	Bare	19	Top diffusers
42	FC/PC	FC/PC	103	Deck
42	FC/PC	Bare	19	Bottom diffusers
1	FC/PC	Bare	122	Crate to monitor PMT(s)
0.21	FC/PC	Bare	122	Crate internal patch 1
0.18	FC/PC	Bare	122	Crate internal patch 2

[†]Staged approach:

32	FC/PC	Bare	24	Barrel (levels 1+2)
58	FC/PC	Bare	36	Barrel (levels 3+4+5)
76	FC/PC	Bare	24	Barrel (levels 5+6+7)

Table XIV: List of all required fibres for the LED system with necessary lengths, connector configurations, quantities and uses.

840 10 Photon Yield Requirements

841 With a series of points in the system where light can be lost, it is important to verify the number
 842 of photons required to be injected into the tank for calibration, and the initial laser power required
 843 to achieve this. This section describes the study performed to calculate these required numbers.

844 A series of simulations were run using the Monte Carlo generation package for Hyper-K, WCSim
 845 [25], using diffusers at each vertical depth level (injector indices 0, 4, 8, 12, 16, 20, 24), along with
 846 one on the top end cap (28) and one on the bottom (32). For each injector, sets of simulations were
 847 run with injected light at wavelengths of 365 nm, 395 nm, 415 nm, 465 nm, 496 nm and 525 nm.
 848 These are a subset of the wavelengths used for attenuation measurements in Section 4.3.1 and,
 849 although not necessarily the exact wavelengths that will be used in the system, allow for explicit
 850 calculation of loss factors due to attenuation without interpolating between measurements. Within
 851 each of these sets, a number of simulations were run at differing values of injected photons, initially
 852 increasing in steps of 200, before moving to larger steps for the higher wavelengths which required
 853 greater numbers. For all simulations, 1000 events are run, using nominal water parameters. The
 854 injector is treated as an ideal diffuser, with a 40° opening half-angle, and dark noise was disabled.

855 The aim for general running of the diffusers is 1% PMT coverage within the diffuser spot, and
 856 so this is used as the target for these studies. For each of the 1000 events in a simulation, the
 857 number of hit PMTs within the diffuser spot is calculated and histogrammed. This is fit with a
 858 Gaussian distribution, and the mean of that taken to be the number of hit PMTs within the spot.
 An example of this distribution is shown in Figure 23. The obtained mean can then be compared

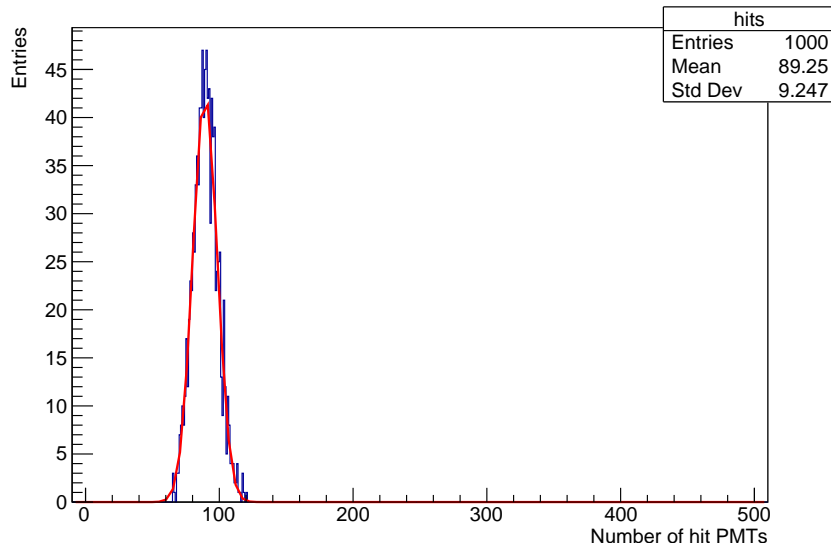


Figure 23: Number of hit PMTs in the spot of diffuser 0, for 1000 injected photons at a wavelength of 365 nm.

859
 860 to the total number of PMTs within the diffuser spot, to calculate the percentage coverage. This
 861 is repeated for all simulations, and compared to the 1% requirement for all injectors to obtain the
 862 minimum number of injected photons required.

863 The coverage percentages for all nine injectors for the 365 nm wavelength are given in Figure 24.
 864 The shape of these plots can be understood by thinking about the geometry of the detector.
 865 Injectors 0 and 24 are the barrel injectors closest to the bottom and top endcaps respectively, so

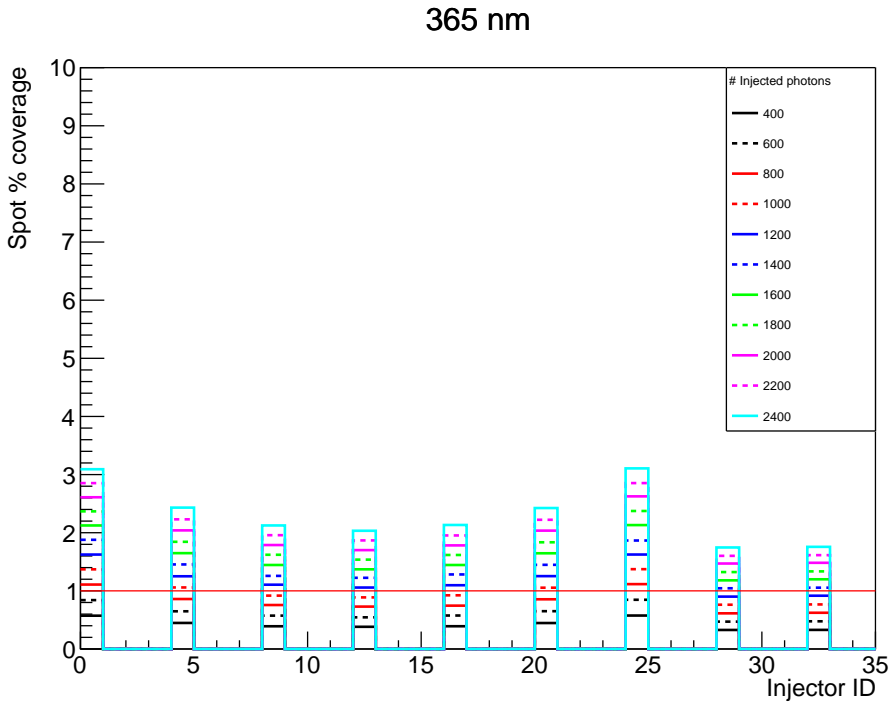


Figure 24: Coverage percentages as a function of diffuser position, for differing numbers of injected photons of 365 nm wavelength. The 1% level is shown by the red line.

those diffusers illuminate a large part of the respective end caps. The shorter path lengths between these injectors and the endcaps results in a greater amount of the initial photons causing hits, and therefore less required for 1% coverage. As the injector positions move towards the middle, there is less to no overlap with the end caps, increasing the average path length to PMTs. The final two injectors, those on the top and bottom end caps, have the greatest distance to the opposite side of the tank. There are therefore more PMTs in the spot, and with the greater distance photons are required to travel, means a greater number of injected photons are needed for 1% coverage. At this wavelength, 1400 injected photons are required to obtain at least 1% coverage in all injectors. The behaviour described repeats for all wavelengths checked, making the top and bottom injectors the limiting cases for each.

The approximate number of photons required to achieve 1% spot coverage per wavelength is given in Table XV. These numbers can then be used to calculate the required laser power per wavelength, accounting for loss due to attenuation in the fibres and other points of inefficiency within the system. The attenuation coefficients calculated in Section 4.3.1 for the above wavelengths are used to obtain the attenuation factors for the fibres, assuming the 175 m calculated in Section 9. The fibre is assumed to be the Thorlabs FG105UCA favoured in Section 4.5.

Additional light loss factors are also added into the calculations. A 90% loss is included to account for the efficiency of the ID diffuser. To account for losses in the fibre switch, we use the worst case scenario from the Weinert FP400URT measurements, and assume a 25% loss at each stage of the switch. As any larger switch is formed by daisy-chaining 1x4 switches, this 25% loss can be experienced up to 6 times (twice for a 1x8 switch plus four times for a 1x80 switch), resulting in an efficiency of $0.75^6 \simeq 0.18$. As the Weinert GIF50C results showed much greater transmission

Wavelength (nm)	N photons for 1% coverage
365	1400
395	1200
415	2000
465	3000
496	6000
525	24000

Table XV: Approximate number of injected photons required for 1% diffuser spot coverage, per wavelength.

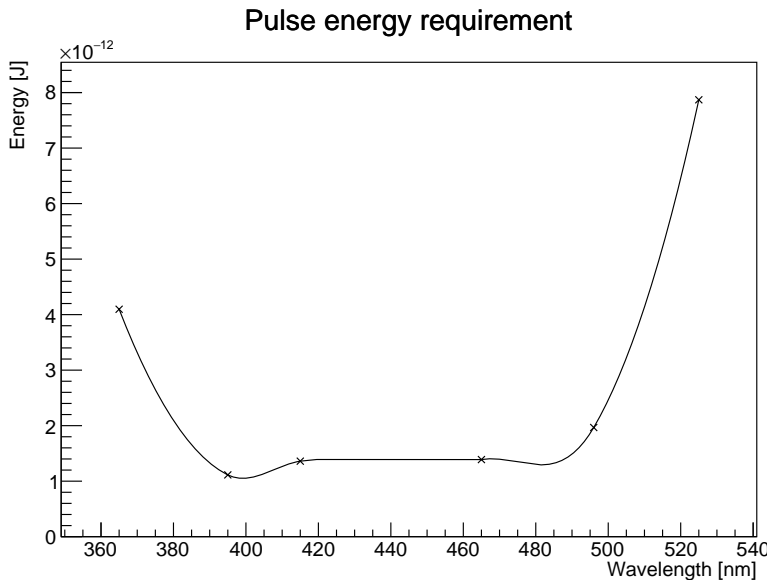


Figure 25: Laser pulse energy as a function of wavelength required to achieve 1% diffuser spot coverage.

these numbers are considered conservative, and the final efficiency of the device will depend on the internal fibre used. Finally, a factor of 50% is included to account for any losses in coupling fibres together across the system.

Applying these scaling factors to the requirements in Table XV yields the required number of photons per pulse from the laser, which goes up to at most 2.4×10^5 at 525 nm. This can easily be translated to the required energy per pulse, which is given in Figure 25. Finally, assuming a 1 kHz pulse frequency for occasional intensive calibration runs, the average power required of the lasers at each wavelength is given in Figure 26.

11 Summary

This technical note describes the tests performed on candidate fibre optic cables, which are used to justify the choices made for optimal fibres to use for the ID and OD systems. For the ID system, along with the OD collimators, Thorlabs FG105UCA is chosen. This fibre showed the least attenuation of the four types tested, in the UV wavelength range which is of most interest, and also matches the fibre type that has already been chosen as the internal feed-through for the optics themselves. This reduces losses that would otherwise be obtained when coupling fibres of

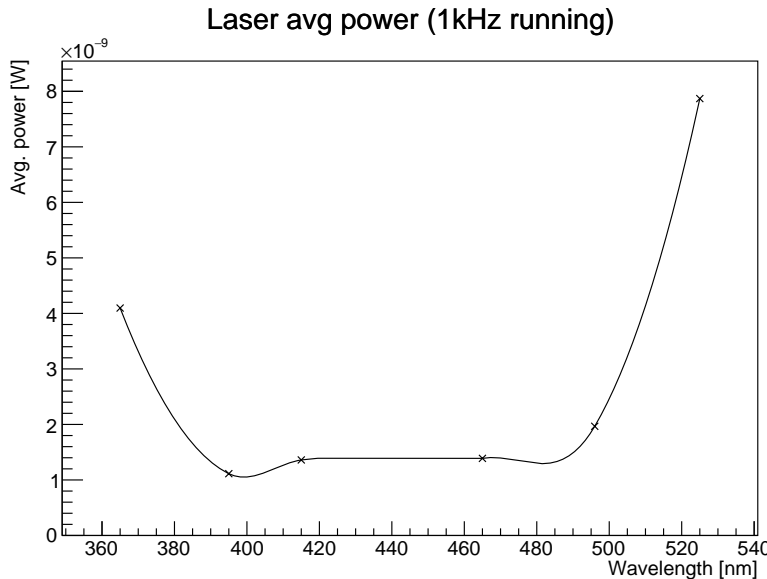


Figure 26: Laser average power as a function of wavelength required to achieve 1% diffuser spot coverage, for 1 kHz running.

903 different types together. This is the reason for choosing this fibre, despite the fact it exhibits a
 904 greater increase in pulse rise time than the other candidates. A high frequency read-out system is
 905 currently in development in order to make complete measurements of the dispersion from the full
 906 lengths of this fibre, as this is still an important property to understand.

907 For the OD diffuser system, the fibre if choice is instead Thorlabs FP400URT. While this
 908 showed increased attenuation at lower wavelengths when compared to FG105UCA, the advantage
 909 of the former fibre type is the diameter being four times greater. This makes coupling an LED to
 910 the fibre considerably easier, and ensures a greater amount of light is directed into the fibre in the
 911 first place.

912 A series of measurements of 1x4 fibre switching devices have also been presented, manufactured
 913 by two different companies. The results for power transmission found the Weinert device with
 914 GIF50C internal fibre to be the best, while for power variation the Agiltron FP400URT device
 915 performed slightly better than the others. However, when making power measurements, none-
 916 zero power measurements were observed on channels of the Agiltron device that were not being
 917 illuminated. Dedicated measurements of this showed cross talk between several different channels
 918 on the Agiltron device, whereas no measurable cross talk was found for either of the Weinert
 919 devices. Coupled with the fact the support from Weinert was vastly superior, which will be
 920 incredibly important for maintaining the device over the lifetime of the experiment, the favoured
 921 company is Weinert. The internal fibre will be the same as that used for the ID laser system, and
 922 as such should be FG105UCA, as discussed already.

923 References

- 924 [1] S. Boyd *et al.*, Hyper-Kamiokande Light Injector Diffuser Technical Note (HK-TN-0042)
- 925 [2] S. Boyd *et al.*, Hyper-Kamiokande Light Injector Collimator Technical Note (HK-TN-0065)
- 926 [3] PicoQuant GmbH, PicoQuant, <https://www.picoquant.com>
- 927 [4] PicoQuant GmbH, Sepia PDL 828 Multichannel Picosecond Diode Laser Driver, September
928 2021, https://www.picoquant.com/images/uploads/downloads/7920-sepia_pdl828.pdf
- 929 [5] PicoQuant GmbH, LDH Series Picosecond Laser Diode Heads for PDL 800-D/PDL 828,
930 January 2024, https://www.picoquant.com/images/uploads/downloads/datasheet_ldh_
931 series.pdf
- 932 [6] PicoQuant GmbH, LDH-FA Series Amplified Picosecond Pulsed Laser Diode Heads, Septem-
933 ber 2022, https://www.picoquant.com/images/uploads/downloads/18-ldh-fa-series_
934 3.pdf
- 935 [7] Thorlabs Inc., FP200URT Specifications, 6th February 2024, <https://www.thorlabs.com/>
936 thorproduct.cfm?partnumber=FP200URT
- 937 [8] Thorlabs Inc., FP400URT Specifications, 6th December 2022, <https://www.thorlabs.com/>
938 thorproduct.cfm?partnumber=FP400URT
- 939 [9] Thorlabs Inc., FG050UGA Specifications, 22nd April 2024, <https://www.thorlabs.com/>
940 thorproduct.cfm?partnumber=FG050UGA
- 941 [10] Thorlabs Inc., FG105UCA Specifications, 22nd April 2024, <https://www.thorlabs.com/>
942 thorproduct.cfm?partnumber=FG105UCA
- 943 [11] Thorlabs Inc., GIF50C Specifications, 6th February 2024, <https://www.thorlabs.com/>
944 thorproduct.cfm?partnumber=GIF50C
- 945 [12] Thorlabs Inc., GIF50D Specifications, 6th February 2024, <https://www.thorlabs.com/>
946 thorproduct.cfm?partnumber=GIF50D
- 947 [13] Thorlabs Inc., Optical Power Meter PM100USB Operation Manual v1.7, 28th March 2023,
948 <https://www.thorlabs.com/thorproduct.cfm?partnumber=pm100usb>
- 949 [14] Thorlabs Inc., Fiber Power Head with Silicon Detector S150C, 4th February 2016, <https://www.thorlabs.com/thorproduct.cfm?partnumber=S150C>
- 951 [15] Hamamatsu Photonics K.K., Photomultiplier Tube Modules H10720/H10721 Se-
952 ries, September 2024, <https://www.hamamatsu.com/content/dam/hamamatsu-photonics/>
953 sites/documents/99_SALES_LIBRARY/etd/H10720_H10721 TPM01062E.pdf
- 954 [16] Tektronix Inc., 5 Series MSO Mixed Signal Oscilloscope Datasheet, <https://www.tek.com/en/datasheet/5-series-mso>
- 956 [17] Y. Nishimura, The Box-and-Line PMT (R12860), (HK-TN-0009 Ver.1.2 RevId20200718)

- 957 [18] Thorlabs Inc., ADAFC1 - FC/PC to FC/PC Mating Sleeve, Wide Key (2.2 mm), D-Hole,
958 <https://www.thorlabs.com/thorproduct.cfm?partnumber=adafc1>
- 959 [19] Thorlabs Inc., FT030-BK - Black Reinforced Ø3 mm Furcation Tubing, <https://www.thorlabs.com/thorproduct.cfm?partnumber=FT030-BK>
- 961 [20] K. Abe *et al.*, Second gadolinium loading to Super-Kamiokande, NIM A 1065 (2024), <https://doi.org/10.1016/j.nima.2024.169480>
- 962
- 963 [21] Agiltron, <https://agiltron.com>
- 964 [22] Weinert Industries, <https://weinert-industries.com/en/>
- 965 [23] TREND Networks FibreMaster MM 850nm Light Source, <https://www.trend-networks.com/product/cable-tester-fibermaster/>
- 966
- 967 [24] Far Facility Working Group, Water tank and PMT support structure (HK-TN-0048)
- 968 [25] WCSim, <https://github.com/WCSim/WCSim>

969 **A Additional Cross Talk Plots**

970 **A.1 Weinert FP400URT**

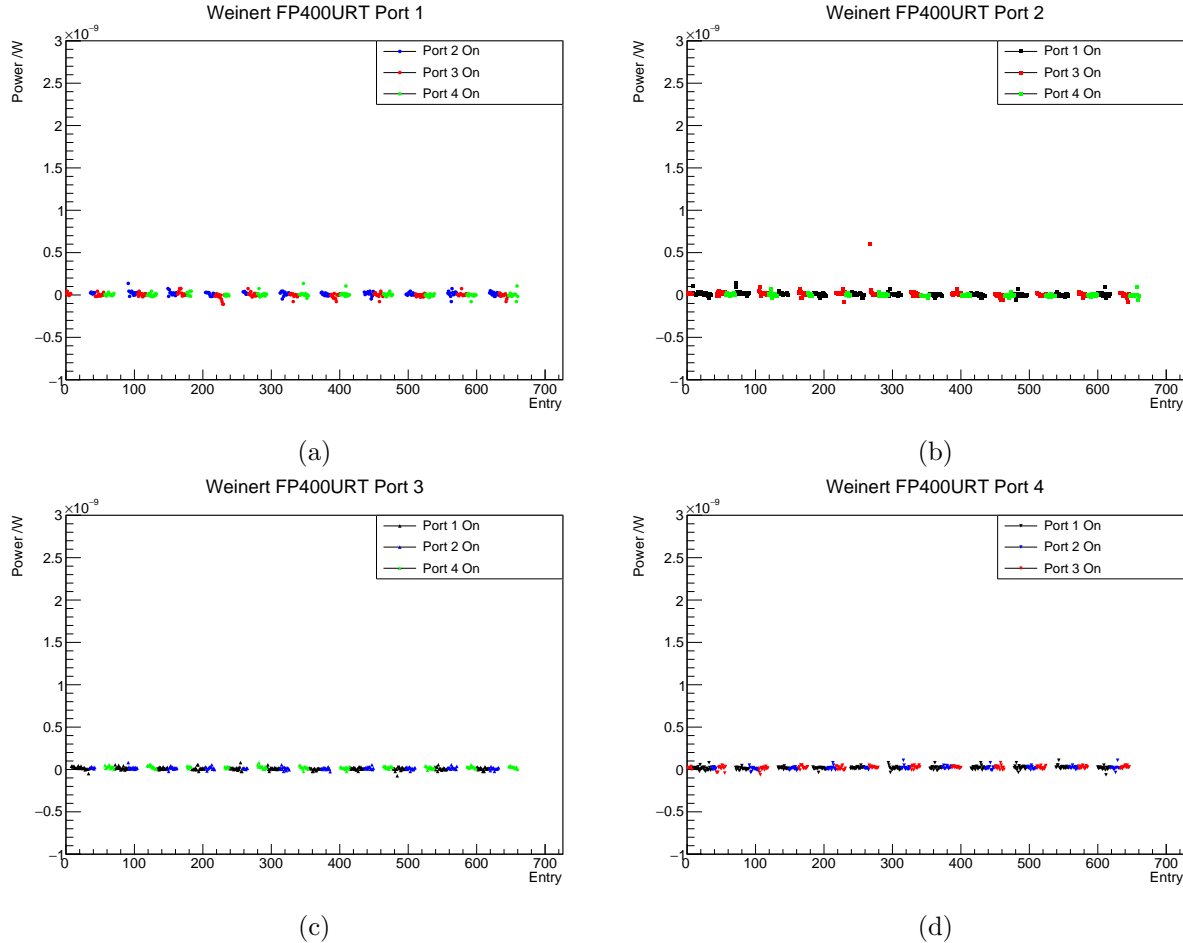


Figure 27: Power recorded on a) port 1, b) port 2, c) port 3 and d) port 4 of the Weinert FP400URT switch, when one of the other three ports was illuminated.

971 A.2 Weinert GIF50C

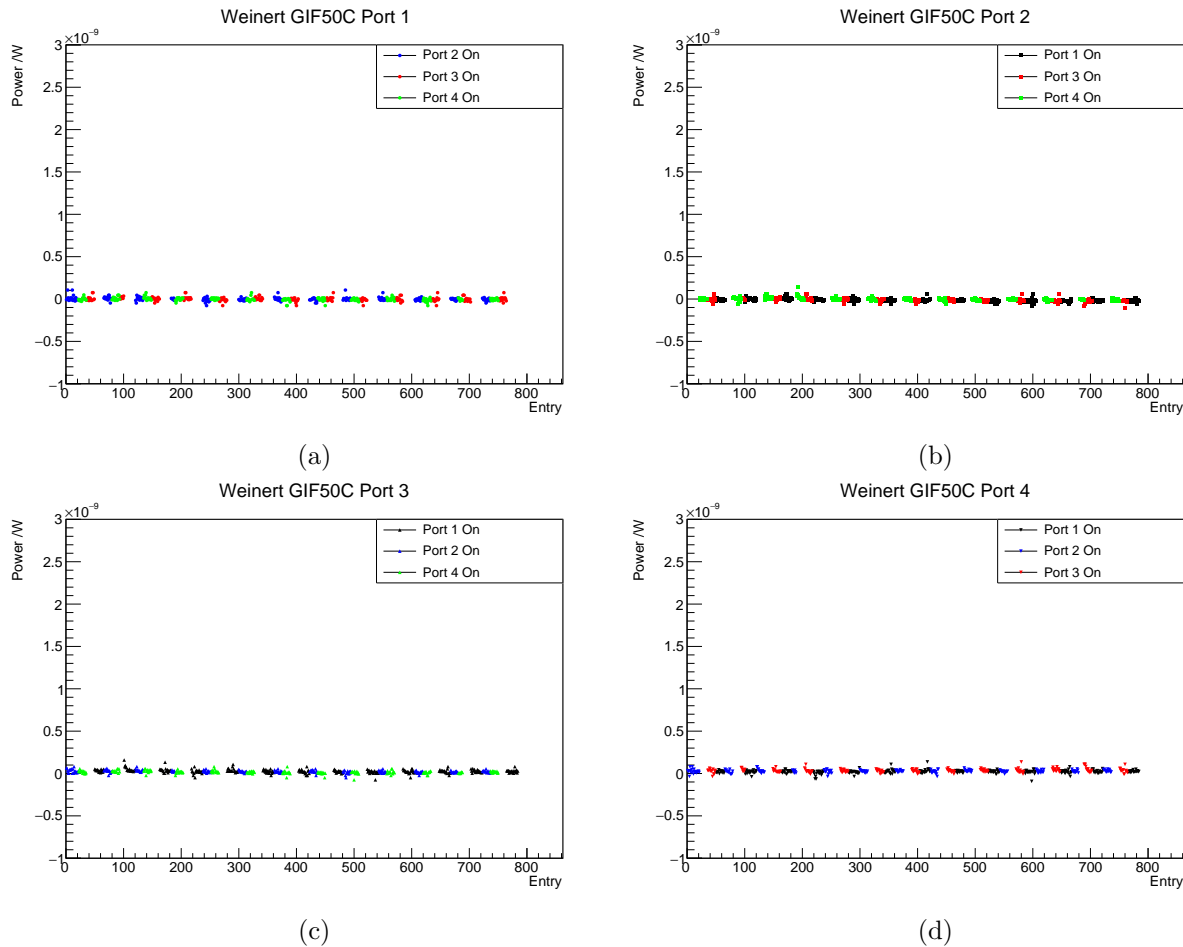


Figure 28: Power recorded on a) port 1, b) port 2, c) port 3 and d) port 4 of the Weinert GIF50C switch, when one of the other three ports was illuminated.

972 **B Fibre Configuration**

973 A more detailed breakdown of the required fibres for both the laser and LED systems is given in
974 Table XVI and Table XVII respectively.

Length [m]	Connector A	Connector B	Req. no.	Fibre location	Injector use
76	FC/PC (air)	FC/PC (water)	56	Barrel	Barrel ID (all) [†]
76	FC/PC (air)	FC/PC (water)	8	Barrel	Bottom ID
76	FC/PC (air)	FC/PC (water)	9	Barrel	Bottom edge OD collimators
42	FC/PC (air)	FC/PC (air)	56	Deck	Barrel ID
42	FC/PC (air)	FC/PC (air)	8	Deck	Bottom ID
42	FC/PC (air)	FC/PC (air)	12	Deck	All OD collimators
42	FC/PC (water)	FC/PC (water)	8	Bottom	Bottom ID
10	FC/PC (air)	FC/PC (water)	2	Top	Top ID
10	FC/PC (air)	FC/PC (water)	3	Top	Top edge OD collimators
1	FC/PC (air)	FC/PC (air)	8	Laser system	Before channel split
0.64	FC/PC (water)	FC/PC (water)	28	Barrel (dead region)	ID diffuser patch cable
0.64	FC/PC (water)	FC/PC (water)	4	Bottom (dead region)	ID diffuser patch cable
0.56	FC/PC (water)	FC/PC (water)	28	Barrel (dead region)	ID collimator patch cable
0.56	FC/PC (water)	FC/PC (water)	4	Bottom (dead region)	ID collimator patch cable

[†] Staged approach:

32	FC/PC (air)	FC/PC (water)	16	Barrel	Barrel ID (levels 1+2)
58	FC/PC (air)	FC/PC (water)	24	Barrel	Barrel ID (levels 3+4+5)
76	FC/PC (air)	FC/PC (water)	16	Barrel	Barrel ID (levels 6+7)

Table XVI: [List of all required fibres for the laser system with necessary lengths, connector configurations and quantities, along with the location the fibres will be installed and the injectors requiring them. Connector A\(B\) is defined as that closest to \(furthest from\) the light source.](#)

Length [m]	Connector A	Connector B	Req. no.	Fibre location	Injector use
76	FC/PC (air)	FC/PC (water)	19	Barrel	Bottom OD diff.
76	FC/PC (air)	Bare (water)	84	Barrel	Bottom OD diff. (all) [†]
50	FC/PC (air)	Bare (water)	19	Top	Top OD diff.
42	FC/PC (air)	FC/PC (air)	19	Deck	Bottom OD diff.
42	FC/PC (air)	FC/PC (air)	84	Deck	Barrel OD diff.
42	FC/PC (air)	Bare (water)	19	Bottom	Bottom OD diff.
1	FC/PC (air)	Bare (air)	122	Crate	Monitor PMT(s)
0.21	FC/PC (air)	Bare (air)	122	Crate	Internal patch 1
0.18	FC/PC (air)	Bare (air)	122	Crate	Internal patch 2

[†] Staged approach:

32	FC/PC (air)	Bare (water)	24	Barrel	Barrel (levels 1+2)
58	FC/PC (air)	Bare (water)	36	Barrel	Barrel (levels 3+4+5)
76	FC/PC (air)	Bare (water)	24	Barrel	Barrel (levels 6+7)

Table XVII: List of all required fibres for the LED system with necessary lengths, connector configurations, quantities, along with the location the fibres will be installed and the injectors requiring them. Connector A(B) is defined as that closest to (furthest from) the light source.